The SKA3-DUSP2 Axis Promotes Gastric Cancer Tumorigenesis and Epithelial-Mesenchymal Transition by Activating the MAPK/ERK Pathway

Chao Zhang
China Medical University First Hospital
Songcheng Yin
China Medical University First Hospital
Yuen Tan
China Medical University First Hospital
Siwei Pan
China Medical University First Hospital
Wen An
China Medical University First Hospital
Qingchuan Chen
China Medical University First Hospital
Huimian Xu (xuhuimian1952@163.com)
China Medical University First Hospital https://orcid.org/0000-0002-1177-4445

Research

Keywords: gastric cancer, SKA3, DUSP2, EMT, MAPK/ERK

Posted Date: November 12th, 2020

DOI: https://doi.org/10.21203/rs.3.rs-103655/v1

Version of Record: A version of this preprint was published at Frontiers in Pharmacology on February 28th, 2022. See the published version at https://doi.org/10.3389/fphar.2022.777612.

Abstract

Background: Spindle and kinetochore-related complex subunit 3 (SKA3), a member of the SKA family of proteins, is associated with the progression of multiple cancers. However, the role of SKA3 in gastric cancer has not been studied.

Methods: The expression levels of SKA3 and dual-specificity phosphatase 2 (DUSP2) proteins were detected by immunohistochemistry. The effects of SKA3 and DUSP2 on the proliferation, migration, invasion, adhesion, and EMT of gastric cancer were studied in vitro and in vivo.

Results: Immunohistochemical analysis of 164 cases of gastric cancer revealed that high expression of SKA3 was negatively correlated with DUSP2 expression and related to N stage, peritoneal metastasis, and poor prognosis. In vitro studies showed that silencing SKA3 expression inhibited the proliferation, migration, invasion, adhesion and EMT of gastric cancer. In vivo experiments showed that silenced expression of SKA3 inhibited tumor growth and peritoneal metastasis. Mechanistically, we found that SKA3 regulates the tumor suppressor DUSP2 and activates the MAPK/ERK pathway to promote gastric cancer.

Conclusions: The SKA3-DUSP2-ERK1/2 axis is involved in the regulation of gastric cancer progression, and SKA3 is a potential therapeutic target for gastric cancer.

Background

Gastric cancer (GC) has a high morbidity and mortality rate worldwide. Although GC patients can benefit from surgery and chemoradiotherapy, the 5-year survival rate is only 40% [1, 2]. Patients with GC mostly die from metastasis and recurrence after surgery, and therefore learning the progression of invasion and metastasis of GC is critical to identify an effective treatment target.

Spindle and kinetochore related complex subunit 3 (SKA3) is a newly discovered important factor involved in the formation of Spindle and moving-particle related complex (SKA), located on chromosome 13q12.11, which controls mitosis together with the NDC80 complex [3–7]. Recent studies showed that SKA3 can not only affect the proliferation of tumor cells by regulating cell cycle checkpoints, but also participate in a variety of cell biological functions to affect the occurrence and development of tumors, thus playing a cancer-promoting role [8–11].

Dual-specific phosphatase 2 (DUSP2) is a member of the tyrosine-specific phosphatase family [12, 13], which contains more than 30 DUSP proteins. DUSP2 is not only an important regulator of immune responses, but its low expression has been detected in various tumors, such as prostate cancer, glioma, and leukemia. DUSP2 participates in the development of tumor regulation through multiple signaling pathways and negatively regulates the activity of extracellular regulatory protein kinase (ERK) and p38 in vitro [14–16]. However, the role of DUSP2 in GC has not been clarified.

Here we studied the expression and progression of SKA3 in GC in vitro and vivo. Our results identified the SKA3-DUSP2-ERK1/2 axis as a potential therapeutic strategy for GC.

Methods

Patient tissue specimens

Our study included two independent experimental cohorts. The first group included 35 cases of fresh frozen tumors and adjacent tissues selected from January to March 2018 in the First Hospital of Gastrointestinal Tumor Surgery affiliated to the China Medical University, performing quantitative real-time PCR (qRT-PCR) and Western blot analysis. The second group included 164 tissue samples from Gastrointestinal Cancer Surgery Department of the First Affiliated Hospital of China Medical University for radical gastrectomy from March 2009 to June 2012, performing immunohistochemistry for SKA3 and DUSP2. All included patients had a single lesion as confirmed by pathological verification and with complete postoperative follow-up data; the patients did not receive chemoradiotherapy before surgery. The study protocol was approved by the hospital ethics committee, and all patients signed informed consent.

Immunohistochemistry

After dewaxing and hydration, paraffin-embedded sections were immersed in 3% H_2O_2 solution for 20 min at 37°C to eliminate endogenous peroxidase followed by incubation in sodium citrate buffer (pH 6.0) at 121°C for 2 min. Sections were then incubated with primary antibodies against SKA3 (1:200, Abcam, Cambridge, MA, USA) and DUSP2 (1:200, Abcam) at 4°C overnight. Sections were then incubated with secondary antibodies at 37°C for 30 min and then stained with 3, 3-diaminobenzidine and counter-stained with hematoxylin for 1 min. Sections were dehydrated in gradient ethanol series followed by xylene. Samples were scored according to staining intensity and proportion of positive cells. Staining intensity was scored as follows: 0 for colorless, 1 for yellow, 2 for brown, and 3 for dark brown. The proportion of positive cells was scored as follows: < 5% was 0, 5%~25% was 1, 25%~50% was 2, 50%~75% was 3, and > 75% was 4. The final score was the product of the staining intensity and the proportion of positive cells scores; samples with scores ≥ 5 were considered positive and samples with scores ≤ 4 were negative.

Cell culture and transfection

The immortalized gastric epithelium cell line GES-1 and GC cell lines SGC-7901, MGC-803, HGC-27, and MKN-45 were purchased from Cell Bank of the Chinese Academy of Sciences (Shanghai, China). Cells were cultured in DMEM and RPMI 1640 medium containing 10% serum. The human peritoneal mesothelial cell (HPMC) HMrSV5 was provided by Youming Peng (Second Hospital of Zhong nan University, Changsha, China) and cultured in RPMI 1640 medium containing 10% serum. Cells were cultured in an incubator at 37°C in 5% CO2.

SKA3 silencing lentiviruses (sh-SKA3), DUSP2 silencing lentiviruses (sh-DUSP2), DUSP2 overexpression lentiviruses (oe-DUSP2) and empty vector (control) were produced by Genechem (Shanghai, China). GC cells were seeded in 12-well plates and when cells achieved 60% to 70% confluence, an appropriate amount of virus was added according to the cell line MOI value. Stable infected cell lines were selected in 5 μg/mL purinomycin or neomycin. The sequences of sh-SKA3 are follows: sh-1, CTTATGAGAATCTGCTCAGAA and sh-2, GCATAGCTTTGGTATCCACAA. The sequence of sh-DUSP2 is CATCTGTCTGGCATACCTCAT and the control sequence is TTCTCCGAACGTGTCACGT.

Quantitative real-time PCR (qRT-PCR)

GC tissues and cells total RNA was extracted by Trizol reagent (Invitrogen, Carlsbad, CA, USA). cDNA was obtained by reverse transcription reaction using a reverse transcription kit (Takara, Tokyo, Japan), and the SYBR Premix Ex Taq ™ kit (Takara, Japan) was conducted qRT-PCR. The experiment was repeated three times. GAPDH mRNA was used as the internal reference gene. Data expression was determined by the $-\Delta\Delta Ct$ method [17].

The primer sequences for qRT-PCR are as follows.

SKA3 forward: 5'-GCCATAGATACAGAATCCAGGCT-3'

SKA3 reverse: 5'-CCAAAGGAGAGTTGGTATATTCGG-3'

DUSP2 forward: 5'-TGTGGAGGACAACCAGATGGTG-3'

DUSP2 reverse: 5'-GAGGTATGCCAGACAGATGGTG-3'

GAPDH forward: 5'-GTCTCCTCTGACTTCAACAGCG-3'

GAPDH reverse: 5'-ACCACCCTGTTGCTGTAGCCAA-3'

Western blot

Total protein was collected from tissues and cells using lysis buffer. Samples were separated by SDS-PAGE gel electrophoresis and transferred to a PVDF membrane. The membrane was blocked in a 5% skim milk for 1 h. The membrane was then incubated overnight at 4°C with primary antibody, followed by incubation in secondary antibody for 1 h. ECL luminescent solution was used to visualize protein bands. Antibodies against SKA3 (ab118560), DUSP2 (ab137640), GAPDH (ab181602) were purchased from Abcam and antibodies against E-cadherin (#14472), N-cadherin (#13116), Vimentin (#5741) Erk1/2 (#4695), and p-Erk1/2 (#4370) were from Cell Signaling Technology.

Co-immunoprecipitation

HGC-27 cell lysates were incubated with primary antibody (IgG as control) and A/G agarose beads at 4ºC for 6 h. After three washes with IP buffer, samples were analyzed by Western blot.

Cell proliferation and colony formation assay

Cell viability was measured using Cell Counting Kit-8 (CCK8, MedChemExpress, USA). GC cells were seeded at 2×10^3 cells/well in 96-well plates. After continuous culture for 24, 48, 72 and 96 h, 10 μl CCK8 solution was added to each well, and after incubation for 2 h, the absorbance value was measured at 450 nm using the Biotek microplate reader.

For clone formation assays, cells were seeded in 6-well plate (1×10^3 cells/well). After further culture for 14 days, the cells were fixed with paraformaldehyde for 20 min and stained with 0.4% trypan blue for 15 min for clone counting.

Flow cytometry

Cells collected by trypsinization were fixed overnight with 900 μl precooling 75% ethanol at 4ºC. Cells were then rinsed with PBS and then incubated in 300 μl propidium iodide staining solution at 37ºC for 30 min in the dark. Cell cycles were then analyzed by flow cytometry.

Wound-healing, cell migration and invasion assays

For wound-healing experiments, cells were uniformly seeded in a six-well plate. Once cells achieved 80% confluence, a 100 μl pipette tip was used to scratch the cells. The same field of vision was photographed under an inverted microscope at 0 h and 48 h after the scratch, and the scratch width was measured.

For migration experiments, a transwell chamber (8 μm, Corning, USA) was placed in a 24-well plate and cells were seeded into the upper chamber at a density of 2×10^4/well. Serum-free medium (100 μl) was added to the top well, and the lower chamber was filled with 600 μl medium containing 10% serum. After 16 h of culture, the transwell chamber was removed, fixed with paraformaldehyde, and stained with 0.4% trypan blue.

For invasion experiments, 90 μl of diluted matrigel (BD Biosciences, NJ, USA) was added to the upper chamber and then 2×10^4/well cells were also seeded into the upper chamber. The subsequent steps were the same as for the migration experiment.

Adhesion assay

HMrSV5 cells were seeded in a 12-well plate one day in advance and GC cells were seeded in a 6 cm diameter petri dish. Next, 2 μl Calcein-AM (Sigma, USA) was added to GC cells and cells were incubated in the dark for 1 h. Stained GC cells (1×10^4) were then added to each well of the plated HMrSV5 cells. The cells were incubated in the dark for 1 h and then washed. The number of GC cells that adhered to HPMCs was counted under a fluorescence microscope.

Animal experiments

All animal experiments were approved by the Ethics Committee of China Medical University and all operations were in accordance with animal ethics.

The subcutaneous tumor model was performed in 12 BALB/c immunodeficient nude mice (SPF level; 4–5 weeks old, female, and approximately 20 g in weight). The MGC-803 control group and the silence group were injected into 3×10^6 cells respectively in the left and right axillas of nude mice. Tumor volume was measured every three days. After 4 weeks, the subcutaneous tumors were dissected and weighed.

The intraperitoneal metastasis model was established in 20 BALB/c nude mice. Mice were assigned to two groups (n=10 per group), and 5×10^6 MGC-803 control or silent cells were injected into the abdominal cavity. After 6 weeks, mice were killed and dissected. The number of tumors on the peritoneal tissue was observed.

Statistical analysis

Statistical analysis was performed using SPSS 22.0 and GraphPad Prism 7.0. Experiments were repeated three times. Data are expressed as mean ± SD. The unpaired *t* test was used to compare the groups. The chi-square test was used to analyze the relationship between SKA3 expression and clinicopathological factors. The Pearson test was used to analyze the correlation between SKA3 and DUSP2 expression. Survival analysis was performed using the Kaplan–Meier method. Log-rank test calculated the survival differences among different groups and fitted the univariate and multivariate Cox proportional hazards model. $P<0.05$ was considered statistically significant.

Results

SKA3 is highly expressed in GC, negatively correlates with DUSP2 expression and is associated with poor prognosis in GC

We analyzed the expression level of SKA3 mRNA in GC in TCGA (Fig. 1A) and GEO databases(GSE66229) (Fig. 1B) and found that SKA3 was highly expressed in GC in both databases. Analysis of 35 GC samples and adjacent tissues by qRT-PCR (Fig. 1C) and Western blot (Fig. 1D) showed that SKA3 expression was up-regulated in GC samples. SKA3 mRNA (Fig. 1E) and protein expression (Fig. 1F) was examined in GC cell lines SGC-7901, MGC-803, HGC-27 and MKN-45 along with GES-1 cells by qRT-PCR and Western blot. SKA3 mRNA and protein was highly expressed in GC cell lines but not in GES-1 cells.

We next performed immunohistochemistry of 164 GC tumor samples and found that SKA3 and DUSP2 were mainly expressed in the cytoplasm and nucleus (Fig. 1G). The positive expression rates of SKA3 and DUSP2 were 52.44% (86/164) and 45.12% (74/164), respectively. There was a negative correlation between SKA3 expression and DUSP2 expression in GC (Pearson test, $r = -0.535$; $P < 0.001$, Fig. 1H).

SKA3 high expression was significantly correlated with Borrmann type, N stage and peritoneal metastasis (all $P < 0.05$, Table 1). Kaplan–Meier analysis showed that patients with high expression of SKA3 (Fig. 1I)

and low expression of DUSP2 (Fig. 1J) showed a worse overall survival (OS), Kaplan-Meier plotter also showed that high expression of SKA3 correlated with worse OS (Fig. 1K). Cox multivariate analysis further confirmed that Borrmann type, T stage, N stage, peritoneal metastasis and SKA3 high expression were independent prognostic factors for OS (HR = 1.829, 95% CI: 1.187–2.818, $P = 0.005$; HR = 1.950, 95% CI: 1.028–3.702, $P = 0.028$; HR = 2.768, 95% CI: 1.471–5.209, $P = 0.001$; HR = 2.210, 95%CI: 1.125–4.342, $P = 0.021$; HR = 1.542, 95% CI: 1.003–2.372, $P = 0.049$), as shown in Table 2.

Table 1
Relationship between the SKA3 expression and clinical parameter

Variables	SKA3 Expression		*P*
	High(n = 86)	Low(n = 78)	
Age			
60	49	34	0.087
≥ 60	37	44	
Sex			
Male	55	53	0.059
Female	31	25	
Size			
< 5(cm)	21	30	0.052
≥ 5(cm)	65	48	
Differentiation			
Well	8	7	0.753
Moderate	31	24	
Poor	47	47	
Tumor location			
Upper	11	9	0.088
Middle	18	7	
Lower	57	62	
Borrmann type			
EGC+-	38	72	0.001
	48	6	
Invasive depth			
T1-T2	12	16	0.265
T3-T4	74	62	
lymph node metastasis			

Abbreviations: SKA3, Spindle and kinetochore-related complex subunit 3;EGC, Early gastric cancer

Variables	SKA3 Expression		*P*
	High(n = 86)	Low(n = 78)	
N0	14	25	0.018
N1-N3	72	53	
Peritoneal metastasis (M)			
M0	73	76	0.005
M1	13	2	
Lymph vessel tumoremboli			
Absent	58	48	0.430
Present	28	30	
Stage(TNM)			
	3	7	0.491
	20	17	
	54	48	
	9	6	
Abbreviations: SKA3, Spindle and kinetochore-related complex subunit 3;EGC, Early gastric cancer			

Table 2
The univariate and multivariate analyses of factors associated with overall survival

Variable	univariate Cox regression		multivariate Cox regression	
	HR (95% CI)	P-value	HR (95% CI)	P-value
Age(< 60)	1.028 (0.696–1.519)	0.888		
Sex(male)	1.224 (0.816–1.835)	0.328		
Size(>5cm)	1.937 (1.223–3.067)	0.005		
Differentiation (Poor)	1.011 (0.681–1.503)	0.956		
Tumor location(Middle, low)	0.983 (0.456–2.120)	0.983		
Borrmann type(□)	2.455(1.643–3.669)	< 0.001	1.829(1.187–2.818)	0.005
Invasive depth (T3-T4)	2.607 (1.390–4.889)	0.003	1.950 (1.028–3.702)	0.028
lymph node metastasis (+)	3.204 (1.709–6.006)	< 0.001	2.768 (1.471–5.209)	0.001
Peritoneal recurrence (+)	2.536 (1.310–4.912)	0.006	2.210 (1.125–4.342)	0.021
Lymph vessel tumoremboli(+)	1.126 (0.749–1.693)	0.568		
High SKA3 expression	1.926 (1.284–2.890)	0.002	1.542 (1.003–2.372)	0.049
Abbreviations: SKA3, Spindle and kinetochore-related complex subunit 3				

SKA3 promotes proliferation, migration, invasion and adhesion of GC cells

High SKA3 expression was detected in MGC-803 and HGC-27 cells, and these cell lines were selected to generate cells with lentivirus-mediated stable knock-down of SKA3 (MGC-803-shSKA3 and HGC-27-shSKA3). Cells infected with lentivirus expressing control were designated as shNC. qRT-PCR and Western blot were used to confirm knock-down efficiency (Fig. 2A).

CCK-8 cell proliferation assay showed that the viability of cells silenced for SKA3 was significantly lower than that of the control group (Fig. 2B). Cloning assays showed that the number of cell clones in the SKA3-silenced cell group was less than that in the control group ($P < 0.05$) (Fig. 2C). Flow cytometry revealed that cells silenced for SKA3 exhibited a cell cycle arrest in G0/G1 phase (Fig. 2D). Wound-healing experiments showed that silencing SKA3 expression inhibited wound-healing (Fig. 3A, E). Transwell migration and invasion experiments showed that silencing SKA3 expression also significantly inhibited the migration and invasion of GC cells (Fig. 3B, C, F, G). We performed immunohistochemical analysis and found that high expression of SKA3 was associated with peritoneal metastasis and we thus carried out adhesion experiments. The number of GC cells silenced for SKA3 that adhered to HPMCs was significantly lower than that in the control group (Fig. 3D, H), indicating that reduced expression of SKA3 resulted in inhibited adhesion ability of GC cells, and made cells less prone to peritoneal metastasis.

Ska3 Regulates Epithelial-mesenchymal Transition (emt) Through Mapk/erk Pathway

Since abnormal activation of EMT is an important biological process in tumor progression, we examined EMT-related markers E-cadherin, N-cadherin and Vimentin in GC cells. Western blot showed that silenced SKA3 resulted in up-regulation of E-cadherin and down-regulation of N-cadherin and Vimentin. The expression of phosphorylated ERK1/2 (Thr202/Tyr204) was also down-regulated in the SKA3 silenced group, while there was no change in overall ERK1/2 level. These results indicate that silenced SKA3 inhibited EMT and the MAPK/ERK pathway (Fig. 4A).

Ska3 Promotes Gc Proliferation And Metastasis In Vivo

We established a subcutaneous tumor model and examined the effects of SKA3 knockdown on tumor growth (Fig. 4B). We found that tumor proliferation was limited in the SKA3 silenced group, and the tumor volumes and weights were smaller than those in the control group (Fig. 4C, D).

We next studied the impact of SKA3 silencing on the metastatic ability of GC using an intraperitoneal metastasis model (Fig. 4E). While extensive and diffuse cancer nodules in the abdominal cavity were observed in the control group, the weight of nodules in the SKA3 silenced group was significantly reduced (Fig. 4F). Together, the results from the in vivo experiments showed that reduced expression of SKA3 inhibited the proliferation, invasion and metastasis of GC.

DUSP2 inhibits MAPK/ERK pathway activity through binding ERK1/2 and inhibits the proliferation, migration, invasion, adhesion and EMT of GC cells

To study the mechanism by which SKA3 promotes the progression of GC, we performed RNA-seq using MGC-803 cells silenced for SKA3 compared with controls. The results showed that 997 genes were upregulated and 236 genes were downregulated. We screened out the downstream gene DUSP2 (Fig. 4G). Previous studies showed that DUSP2 negatively regulates MAPK/ERK and is the upstream gene of MAPK/ERK pathway. Previous studies have reported that the MAPK/ERK pathway plays an important role in the progression of GC [18, 19]. We screened DUSP2 as a key downstream gene through qRT-PCR and Western blot (Fig. 4H, I, J).

We established two stable cell lines overexpressing DUSP2 (MGC-803-oe-DUSP2 and HGC-27-oe-DUSP2), as well as a blank control (oeNC). Western blot was used to confirm overexpression efficiency (Fig. 6A). CCK-8 cell proliferation test showed that the cell proliferation ability of the DUSP2 overexpression group was significantly lower than that of the control group (Fig. 5A). Cloning experiments showed that the number of cell clones in the DUSP2 overexpression group was less than that in the control group ($P < 0.05$) (Fig. 5B). Flow cytometry showed that the DUSP2 overexpression group showed a cell cycle arrest in G0/G1 and G2/M phase (Fig. 5C). Wound-healing experiments showed that DUSP2 overexpression inhibited the migration of GC cells (Fig. 5D). Transwell migration and invasion experiments showed that

DUSP2 overexpression also significantly inhibited the migration and invasion of GC cells (Fig. 5E, F). Using adhesion experiments, we found that the number of GC cells adhering to mesothelial cells in the DUSP2 overexpressed group was significantly lower than that in the control group, indicating that overexpression of DUSP2 inhibited the adhesion ability of GC cells (Fig. 5G). Western blot showed that DUSP2 overexpression resulted in up-regulation of E-cadherin and down-regulation of N-cadherin and Vimentin (Fig. 6A). We performed co-immunoprecipitation experiments and found that DUSP2 binds to ERK1/2, thereby dephosphorylating ERK1/2 and inhibiting MAPK/ERK pathway activity (Fig. 6B).

Knockdown of DUSP2 partially rescued the effects on proliferation and invasion caused by SKA3 knockdown

To verify the SKA3-DUSP2-ERK1/2 signal axis, we co-transfected with shSKA3 and shDUSP2 in the cell line. First, we verified the DUSP2 silenced efficiency (Fig. 6C). We performed functional rescue experiments and found that co-transfected group partially increased cell proliferation (Fig. 6D, E), G0/G1 phase (Fig. 6F), wound-healing (Fig. 7A, E), migration (Fig. 7B, F), invasion (Fig. 7C, G) and adhesion (Fig. 7D, H) compared with SKA3 knockdown cells. Western blot showed that SKA3, N-cadherin, Vimentin, and phosphorylated ERK1/2 expression were partially increased, E-cadherin expression was partially decreased, and total ERK1/2 was unchanged in the double knockdown cells (Fig. 8A). Our study shows that the effect of SAK3 on proliferation and metastasis is likely to be largely achieved through DUSP2, SKA3 negatively regulates DUSP2 and activates the MAPK/ERK pathway to regulate the malignant phenotype of GC (Fig. 8B).

Discussion

The progression of GC is the result of the joint action of a variety of factors. It takes a long time from the initial start to promote the carcinogenesis to the invasion and metastasis. Tumor invasion and metastasis are extremely complex dynamic processes and the most essential feature of malignant tumors. Therefore, experiments of GC focus on exploring potential therapeutic effects of molecular markers through studying the mechanism of invasion and metastasis [20–24].

SKA3 is highly expressed in malignant tumors such as colon cancer, liver cancer and cervical cancer, prostate cancer and plays an important role in cancer occurrence and development [8, 11, 25, 26]. However, the expression of SKA3 in GC and its role in tumorigenesis has been unknown. Our study found that high expression of SKA3 in GC tissues was associated with N stage and peritoneal metastasis, and the patients with high expression of SKA3 was associated with worse prognosis. Chuang et al. found that SKA3 regulates the cell cycle, apoptosis, proliferation and invasion in colorectal cancer and is associated with poor prognosis [25]. Hu et al. found that SKA3 promotes cell proliferation and invasion by regulating the PI3K/Akt pathway in cervical cancer [26]. Our study found that SKA3 activates the MAPK/ERK pathway by regulating DUSP2. We also found that SKA3 promotes GC proliferation and EMT as well as GC invasion and even peritoneal metastasis. This is the first study to reveal the relationship between SKA3 and clinicopathological factors and mechanisms in GC.

When EMT occurs, cell adhesion ability is reduced and migration ability is improved, which in turn induces tumor cells to detach from the primary focus and even infiltrate to distal sites [27–30]. The MAPK/ERK pathway promotes GC cell migration and invasion through EMT. GC cells mediated by the apoptosis factor FAS ligand can inhibit the phosphorylation of GSK-3β through ERK1/2, thereby reducing the degradation of β-catenin by GSK-3β and promoting the accumulation of β-catenin and SNAIL proteins in the nucleus. EMT is thus induced in GC cells. Both β-catenin and SNAIL protein expressions can be blocked by the ERK inhibitor U0126 [31, 32].

DUSP2 is expressed at low levels in a variety of tumors, such as prostate cancer, pancreatic cancer, colon cancer, and leukemia, and participates in the regulation of tumor development through various signaling pathways [19, 33–36]. A previous study showed that DUSP2 negatively regulates ERK and P38 activity in vitro [37]. Our research also confirms that DUSP2 plays a tumor suppressive role in GC and can bind to ERK1/2, thereby promoting its dephosphorylation and inhibiting the MAPK/ERK pathway, resulting in EMT and reduced GC invasion and even peritoneal metastasis. According to the “seed and soil” theory [38], in our study, GC cells generate EMT, which makes them prone to metastasis, while DUSP2 is related to hypoxia [39]. Hypoxia changes the microenvironment of the abdominal cavity. Our adhesion experiments showed that mesothelial cells affected by the changes of microenvironment promote the adhesion ability of GC cells. We have identified a new carcinogenic mechanism involving the SKA3-DUSP2-ERK1/2 axis, but how SKA3 regulates DUSP2 needs to be further explored.

Conclusions

In conclusion, our study found that SKA3 activates the MAPK/ERK pathway by regulating DUSP2, promoting GC proliferation and EMT, and leading to invasion and peritoneal metastasis. As an independent prognostic factor, SKA3 may be a potential therapeutic target and predictive indicator in GC.

Abbreviations

SKA3: Spindle and kinetochore-related complex subunit 3; DUSP2: dual-specificity phosphatase 2; GC: Gastric cancer; ERK: extracellular regulatory protein kinase; qRT-PCR: quantitative real-time PCR; HPMC: human peritoneal mesothelial cell; CCK8: Cell Counting Kit-8; OS: overall survival

Declarations

Acknowledgements

None.

Authors’ contributions

HMX designed the research. CZ took part in designing the research, collected the data, analyzed the date and wrote the manuscript. YET, WA, SWP, QCC collected the data, analyzed the date. SCY solved the

disagreements. All the authors approved the final manuscript.

Conflict of Interest

The authors report no competing interest in this study.

Funding

This work was supported by National Natural Science Foundation of China (No 81772549, 81572334).

Availability of data and materials

All the data reported by the manuscript are publicly available and the materials are also freely available.

Ethics approval and consent to participate

None.

Consent for publication

The corresponding author and all the co-authors agreed to the publication

of the manuscript to this journal.

References

1. Bray F, Ferlay J, Soerjomataram I, Siegel RL, Torre LA, Jemal A. Global cancer statistics 2018: GLOBOCAN estimates of incidence and mortality worldwide for 36 cancers in 185 countries. CA Cancer J Clin. 2018;68:394–424.
2. Noh SH, Park SR, Yang HK, et al. Adjuvant capecitabine plus oxaliplatin for gastric cancer after D2 gastrectomy (CLASSIC): 5-year follow-up of an open-label, randomised phase 3 trial. Lancet Oncol. 2014;15:1389–96.
3. Foley EA, Kapoor TM. Microtubule attachment and spindle assembly checkpoint signalling at the kinetochore. Nat Rev Mol Cell Biol. 2013;14:25–37.
4. Gaitanos TN, Santamaria A, Jeyaprakash AA, Wang B, Conti E, Nigg EA. Stable kinetochore-microtubule interactions depend on the Ska complex and its new component Ska3/C13Orf3. Embo j. 2009;28:1442–52.
5. Ciferri C, Pasqualato S, Screpanti E, et al. Implications for kinetochore-microtubule attachment from the structure of an engineered Ndc80 complex. Cell. 2008;133:427–39.
6. Jeyaprakash AA, Santamaria A, Jayachandran U, et al. Structural and functional organization of the Ska complex, a key component of the kinetochore-microtubule interface. Mol Cell. 2012;46:274–86.
7. Zhang Q, Sivakumar S, Chen Y, et al. Ska3 Phosphorylated by Cdk1 Binds Ndc80 and Recruits Ska to Kinetochores to Promote Mitotic Progression. Curr Biol. 2017;27:1477–84.e4.

8. Hou Y, Wang Z, Huang S, et al. SKA3 Promotes tumor growth by regulating CDK2/P53 phosphorylation in hepatocellular carcinoma. Cell Death Dis. 2019;10:929.
9. Pesson M, Volant A, Uguen A, et al. A gene expression and pre-mRNA splicing signature that marks the adenoma-adenocarcinoma progression in colorectal cancer. PLoS One. 2014;9:e87761.
10. Jiao X, Hooper SD, Djureinovic T, et al. Gene rearrangements in hormone receptor negative breast cancers revealed by mate pair sequencing. BMC Genom. 2013;14:165.
11. Lee M, Williams KA, Hu Y, et al. GNL3 and SKA3 are novel prostate cancer metastasis susceptibility genes. Clin Exp Metastasis. 2015;32:769–82.
12. Low HB, Zhang Y. Regulatory Roles of MAPK Phosphatases in Cancer. Immune Netw. 2016;16:85–98.
13. Caunt CJ, Keyse SM. Dual-specificity MAP kinase phosphatases (MKPs): shaping the outcome of MAP kinase signalling. Febs j. 2013;280:489–504.
14. Lu D, Liu L, Ji X, et al. The phosphatase DUSP2 controls the activity of the transcription activator STAT3 and regulates TH17 differentiation. Nat Immunol. 2015;16:1263–73.
15. Griffin AC 3rd, Kern MJ, Kirkwood KL. MKP-1 is essential for canonical vitamin D-induced signaling through nuclear import and regulates RANKL expression and function. Mol Endocrinol. 2012;26:1682–93.
16. Chu Y, Solski PA, Khosravi-Far R, Der CJ, Kelly K. The mitogen-activated protein kinase phosphatases PAC1, MKP-1, and MKP-2 have unique substrate specificities and reduced activity in vivo toward the ERK2 sevenmaker mutation. J Biol Chem. 1996;271:6497–501.
17. Livak KJ, Schmittgen TD. Analysis of relative gene expression data using real-time quantitative PCR and the 2(-Delta Delta C(T)) Method. Methods. 2001;25:402–8.
18. Wang J, Gui Z, Deng L, et al. c-Met upregulates aquaporin 3 expression in human gastric carcinoma cells via the ERK signalling pathway. Cancer Lett. 2012;319:109–17.
19. Hu J, Li L, Chen H, et al. MiR-361-3p regulates ERK1/2-induced EMT via DUSP2 mRNA degradation in pancreatic ductal adenocarcinoma. Cell Death Dis. 2018;9:807.
20. Wadhwa R, Song S, Lee JS, Yao Y, Wei Q, Ajani JA. Gastric cancer-molecular and clinical dimensions. Nat Rev Clin Oncol. 2013;10:643–55.
21. Van Cutsem E, Sagaert X, Topal B, Haustermans K, Prenen H. Gastric cancer. Lancet. 2016;388:2654–64.
22. Parker BS, Rautela J, Hertzog PJ. Antitumour actions of interferons: implications for cancer therapy. Nat Rev Cancer. 2016;16:131–44.
23. Yang H, Xia L, Chen J, et al. Stress-glucocorticoid-TSC22D3 axis compromises therapy-induced antitumor immunity. Nat Med. 2019;25:1428–41.
24. Hayakawa Y, Ariyama H, Stancikova J, et al. Mist1 Expressing Gastric Stem Cells Maintain the Normal and Neoplastic Gastric Epithelium and Are Supported by a Perivascular Stem Cell Niche. Cancer Cell. 2015;28:800–14.

25. Chuang TP, Wang JY, Jao SW, et al. Over-expression of AURKA, SKA3 and DSN1 contributes to colorectal adenoma to carcinoma progression. Oncotarget. 2016;7:45803–18.
26. Hu R, Wang MQ, Niu WB, et al. SKA3 promotes cell proliferation and migration in cervical cancer by activating the PI3K/Akt signaling pathway. Cancer Cell Int. 2018;18:183.
27. Pastushenko I, Brisebarre A, Sifrim A, et al. Identification of the tumour transition states occurring during EMT. Nature. 2018;556:463–8.
28. Lv ZD, Na D, Liu FN, et al. Induction of gastric cancer cell adhesion through transforming growth factor-beta1-mediated peritoneal fibrosis. J Exp Clin Cancer Res. 2010;29:139.
29. Moreno-Bueno G, Portillo F, Cano A. Transcriptional regulation of cell polarity in EMT and cancer. Oncogene. 2008;27:6958–69.
30. Dongre A, Weinberg RA. New insights into the mechanisms of epithelial-mesenchymal transition and implications for cancer. Nat Rev Mol Cell Biol. 2019;20:69–84.
31. Zheng HX, Cai YD, Wang YD, et al. Fas signaling promotes motility and metastasis through epithelial-mesenchymal transition in gastrointestinal cancer. Oncogene. 2013;32:1183–92.
32. Zheng H, Li W, Wang Y, et al. Glycogen synthase kinase-3 beta regulates Snail and beta-catenin expression during Fas-induced epithelial-mesenchymal transition in gastrointestinal cancer. Eur J Cancer. 2013;49:2734–46.
33. Rohan PJ, Davis P, Moskaluk CA, et al. PAC-1: a mitogen-induced nuclear protein tyrosine phosphatase. Science. 1993;259:1763–6.
34. Yin H, He W, Li Y, et al. Loss of DUSP2 predicts a poor prognosis in patients with bladder cancer. Hum Pathol. 2019;85:152–61.
35. Hou PC, Li YH, Lin SC, et al. Hypoxia-Induced Downregulation of DUSP-2 Phosphatase Drives Colon Cancer Stemness. Cancer Res. 2017;77:4305–16.
36. Hartmann S, Schuhmacher B, Rausch T, et al. Highly recurrent mutations of SGK1, DUSP2 and JUNB in nodular lymphocyte predominant Hodgkin lymphoma. Leukemia. 2016;30:844–53.
37. Dickinson RJ, Keyse SM. Diverse physiological functions for dual-specificity MAP kinase phosphatases. J Cell Sci. 2006;119:4607–15.
38. Paget S. The distribution of secondary growths in cancer of the breast. 1889. Cancer Metastasis Rev. 1989;8:98–101.
39. Karakashev SV, Reginato MJ. Hypoxia/HIF1alpha induces lapatinib resistance in ERBB2-positive breast cancer cells via regulation of DUSP2. Oncotarget. 2015;6:1967–80.

Figures

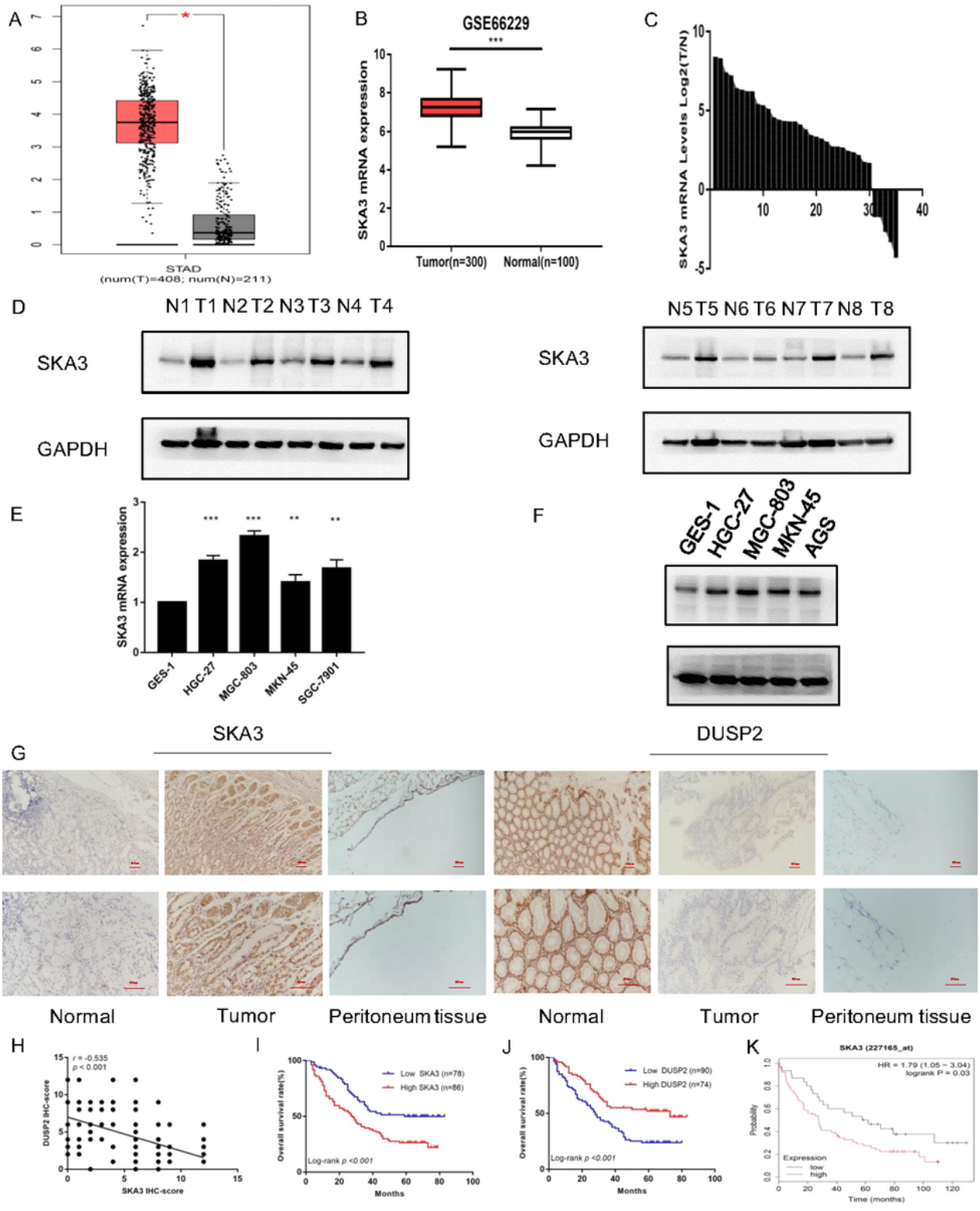

Figure 1

SKA3 is upregulated in gastric cancer. A SKA3 mRNA expression in TCGA database. B SKA3 mRNA expression in GEO database. C SKA3 mRNA expression in gastric cancer tissues. D SKA3 protein levels in gastric cancer tissues. N, normal tissue. T, tumor tissue. E SKA3 mRNA expression in gastric cancer cell lines. F SKA3 protein levels in gastric cancer cell lines. G SKA3 and DUSP2 expression in gastric cancer tissues, normal tissues, peritoneal tissues by immunohistochemistry (IHC). H The correlation between

SKA3 and DUSP2 IHC score by scatter plots. I Kaplan-Meier survival curves about SKA3. J Kaplan-Meier survival curves about DUSP2. K The prognostic significance of SKA3 high and low expression in Kaplan-Meier plotter database. *P < 0.05, **P < 0.01, ***P < 0.001

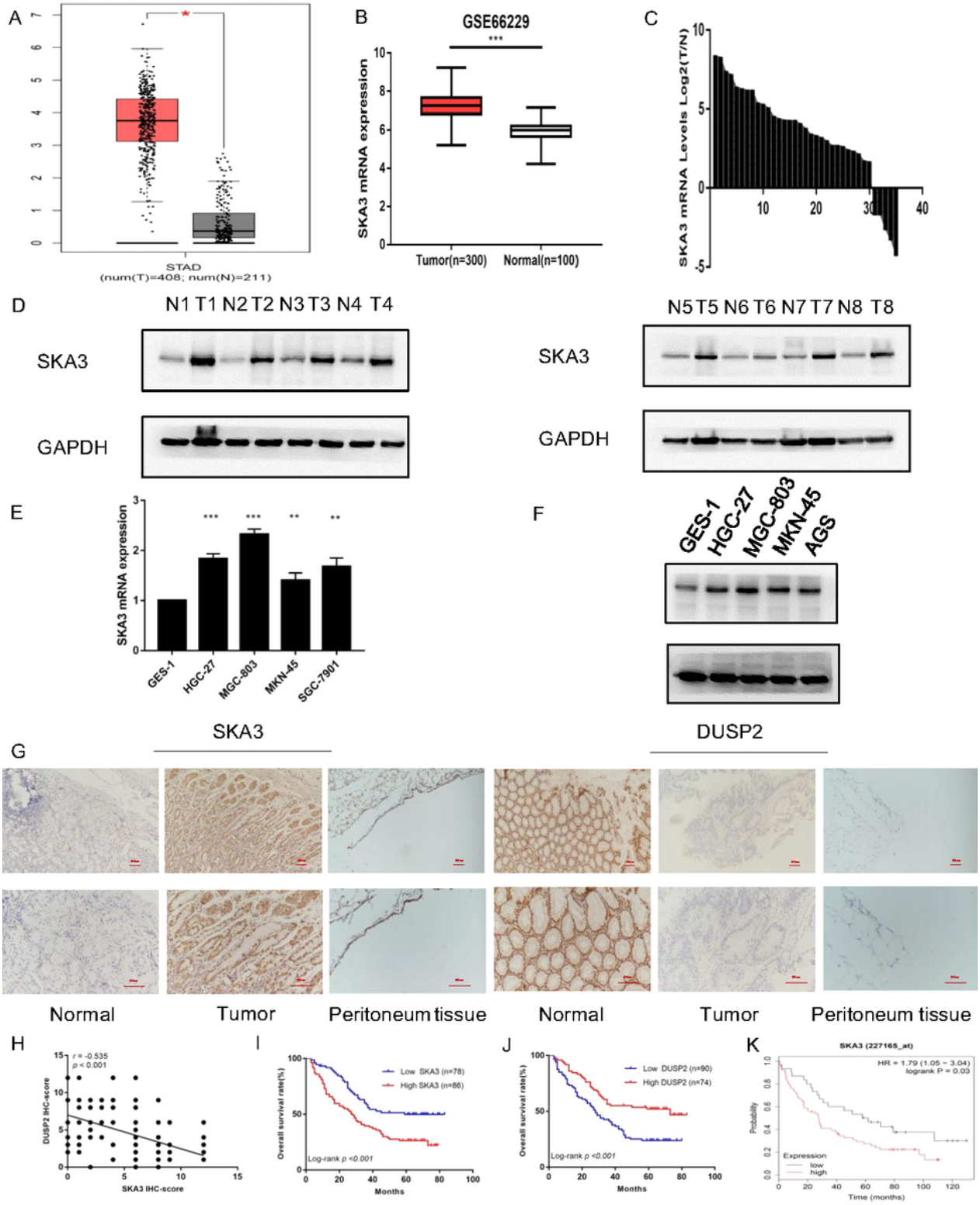

Figure 1

SKA3 is upregulated in gastric cancer. A SKA3 mRNA expression in TCGA database. B SKA3 mRNA expression in GEO database. C SKA3 mRNA expression in gastric cancer tissues. D SKA3 protein levels in

gastric cancer tissues. N, normal tissue. T, tumor tissue. E SKA3 mRNA expression in gastric cancer cell lines. F SKA3 protein levels in gastric cancer cell lines. G SKA3 and DUSP2 expression in gastric cancer tissues, normal tissues, peritoneal tissues by immunohistochemistry (IHC). H The correlation between SKA3 and DUSP2 IHC score by scatter plots. I Kaplan-Meier survival curves about SKA3. J Kaplan-Meier survival curves about DUSP2. K The prognostic significance of SKA3 high and low expression in Kaplan-Meier plotter database. *P < 0.05, **P < 0.01, ***P < 0.001

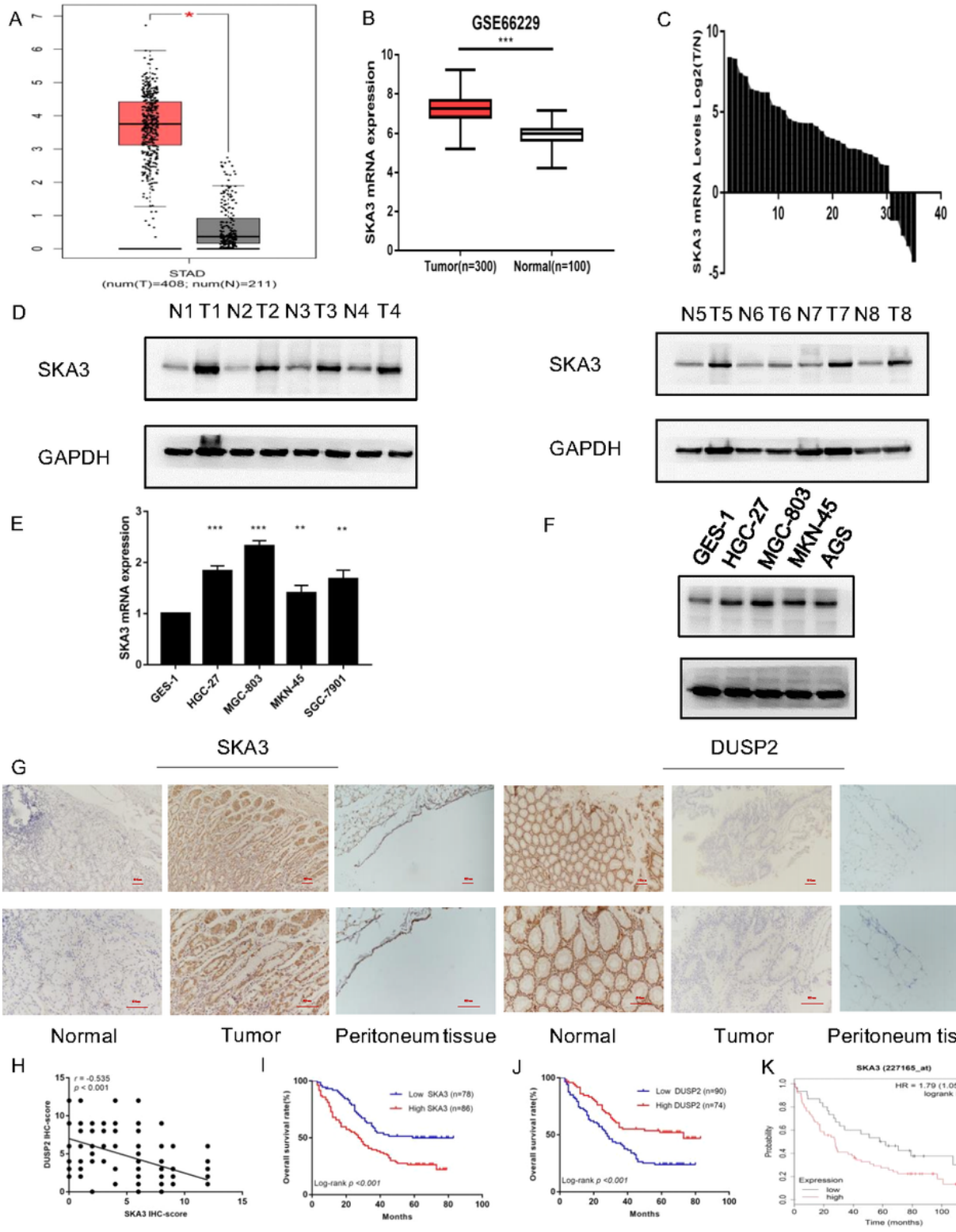

Figure 1

SKA3 is upregulated in gastric cancer. A SKA3 mRNA expression in TCGA database. B SKA3 mRNA expression in GEO database. C SKA3 mRNA expression in gastric cancer tissues. D SKA3 protein levels in gastric cancer tissues. N, normal tissue. T, tumor tissue. E SKA3 mRNA expression in gastric cancer cell lines. F SKA3 protein levels in gastric cancer cell lines. G SKA3 and DUSP2 expression in gastric cancer tissues, normal tissues, peritoneal tissues by immunohistochemistry (IHC). H The correlation between SKA3 and DUSP2 IHC score by scatter plots. I Kaplan-Meier survival curves about SKA3. J Kaplan-Meier survival curves about DUSP2. K The prognostic significance of SKA3 high and low expression in Kaplan-Meier plotter database. *P < 0.05, **P < 0.01, ***P < 0.001

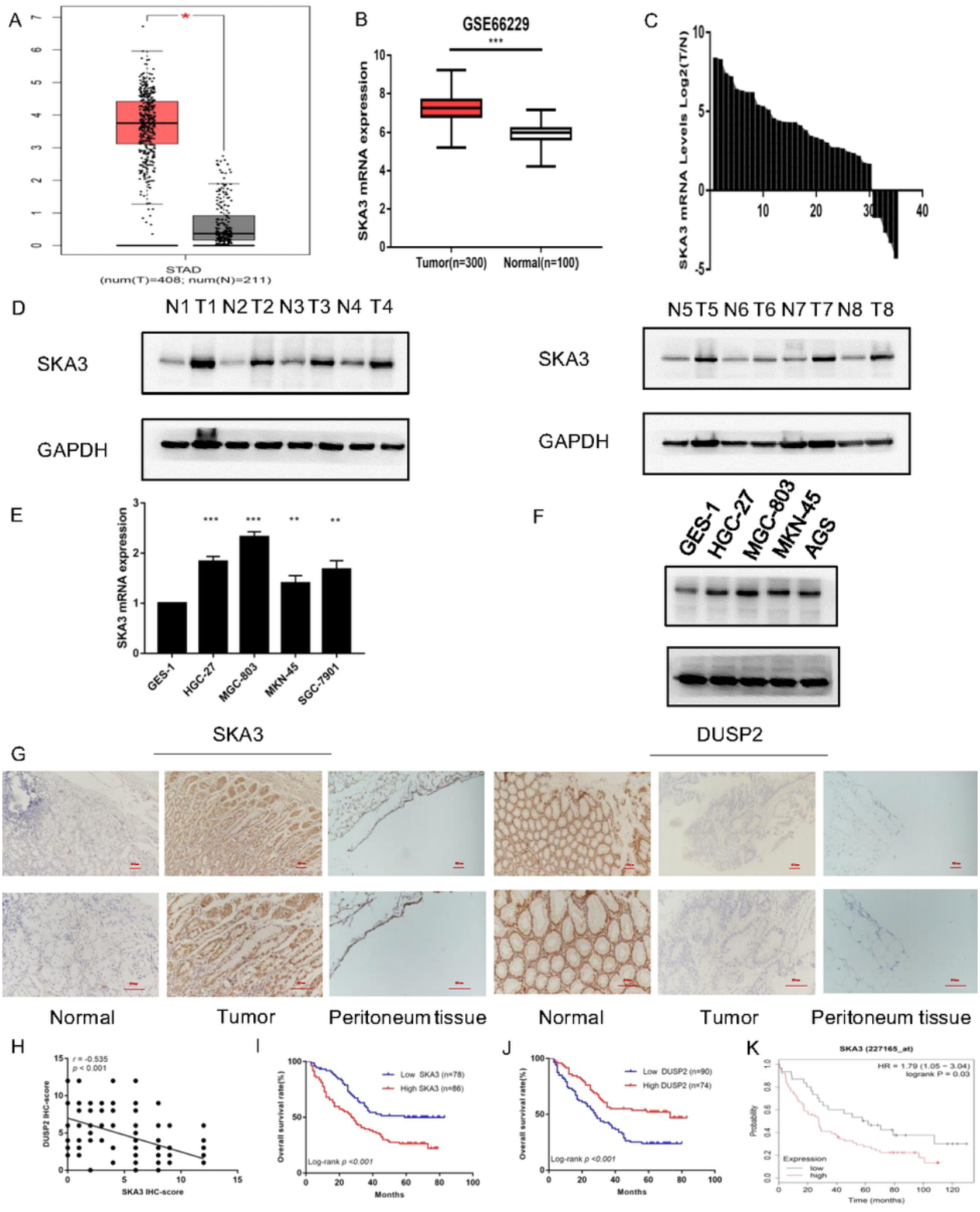

Figure 1

SKA3 is upregulated in gastric cancer. A SKA3 mRNA expression in TCGA database. B SKA3 mRNA expression in GEO database. C SKA3 mRNA expression in gastric cancer tissues. D SKA3 protein levels in gastric cancer tissues. N, normal tissue. T, tumor tissue. E SKA3 mRNA expression in gastric cancer cell lines. F SKA3 protein levels in gastric cancer cell lines. G SKA3 and DUSP2 expression in gastric cancer tissues, normal tissues, peritoneal tissues by immunohistochemistry (IHC). H The correlation between

SKA3 and DUSP2 IHC score by scatter plots. I Kaplan-Meier survival curves about SKA3. J Kaplan-Meier survival curves about DUSP2. K The prognostic significance of SKA3 high and low expression in Kaplan-Meier plotter database. *P < 0.05, **P < 0.01, ***P < 0.001

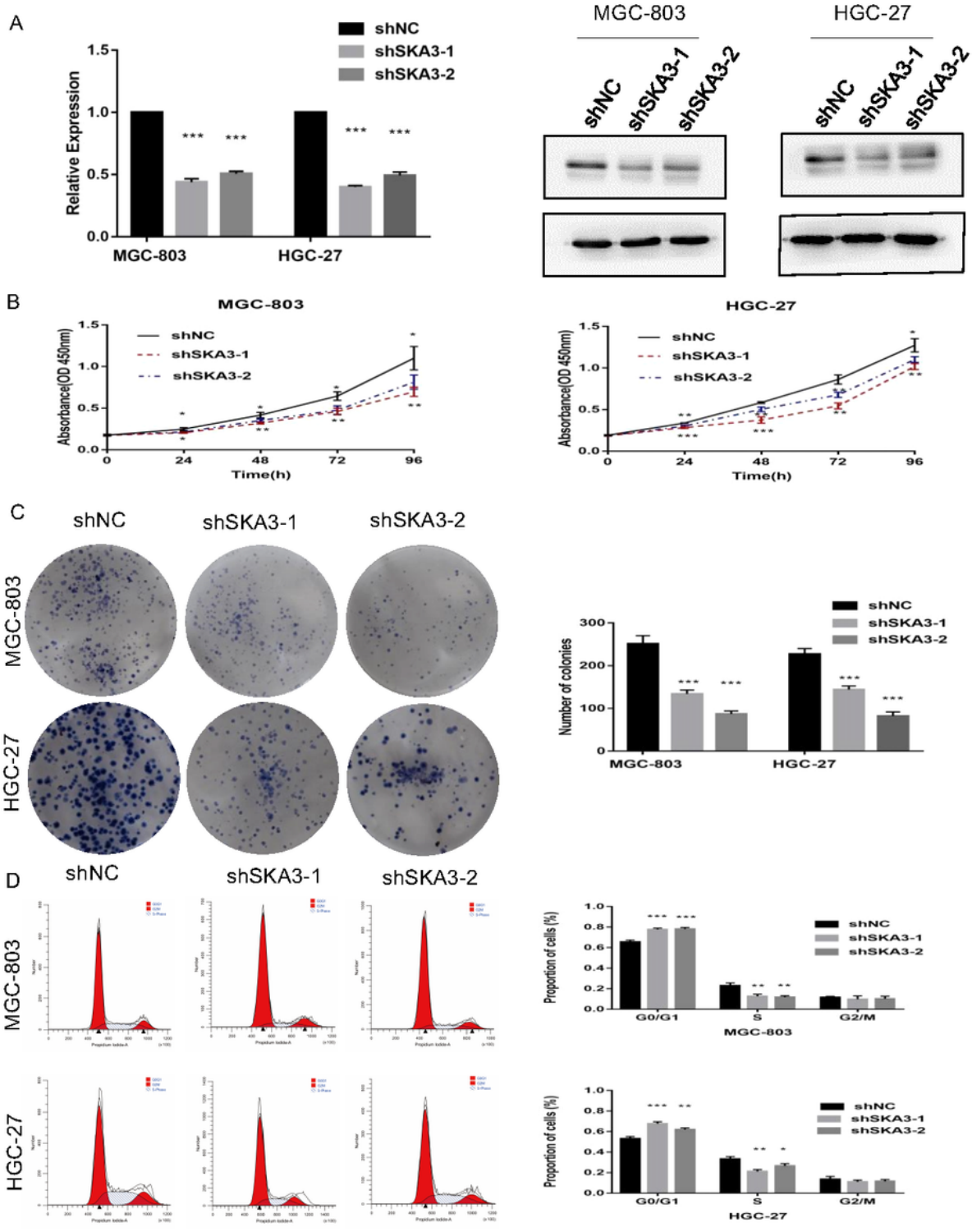

Figure 2

SKA3 promotes proliferation in gastric cancer. A mRNA and protein levels of SKA3 after transfection with shSKA3 lentivirus in MGC-803 and HGC-27. B CCK-8 cell proliferation assay detects cell viability by

silenced for SKA3 in MGC-803 and HGC-27. C Cloning experiment detects cell growth by silenced for SKA3 in MGC-803 and HGC-27. D Flow cytometry detects cell cycle n by silenced for SKA3 in MGC-803 and HGC-27. Data are shown as mean ± SD for triplicate experiments. The two-tailed Student's unpaired t-test was used. *P < 0.05, **P < 0.01, ***P < 0.001

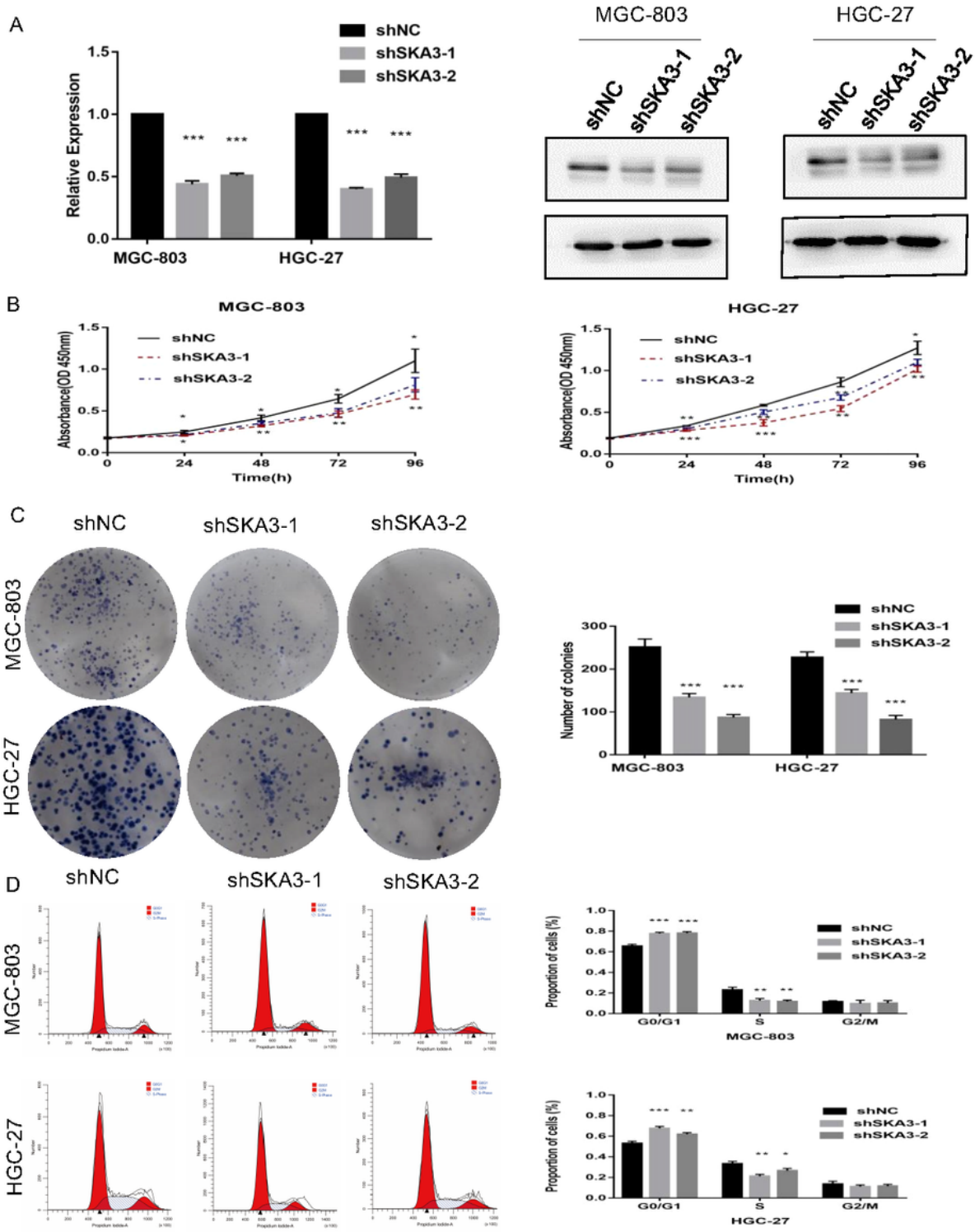

Figure 2

SKA3 promotes proliferation in gastric cancer. A mRNA and protein levels of SKA3 after transfection with shSKA3 lentivirus in MGC-803 and HGC-27. B CCK-8 cell proliferation assay detects cell viability by silenced for SKA3 in MGC-803 and HGC-27. C Cloning experiment detects cell growth by silenced for SKA3 in MGC-803 and HGC-27. D Flow cytometry detects cell cycle n by silenced for SKA3 in MGC-803 and HGC-27. Data are shown as mean ± SD for triplicate experiments. The two-tailed Student's unpaired t-test was used. *P < 0.05, **P < 0.01, ***P < 0.001

Figure 2

SKA3 promotes proliferation in gastric cancer. A mRNA and protein levels of SKA3 after transfection with shSKA3 lentivirus in MGC-803 and HGC-27. B CCK-8 cell proliferation assay detects cell viability by silenced for SKA3 in MGC-803 and HGC-27. C Cloning experiment detects cell growth by silenced for SKA3 in MGC-803 and HGC-27. D Flow cytometry detects cell cycle n by silenced for SKA3 in MGC-803 and HGC-27. Data are shown as mean ± SD for triplicate experiments. The two-tailed Student's unpaired t-test was used. *P < 0.05, **P < 0.01, ***P < 0.001

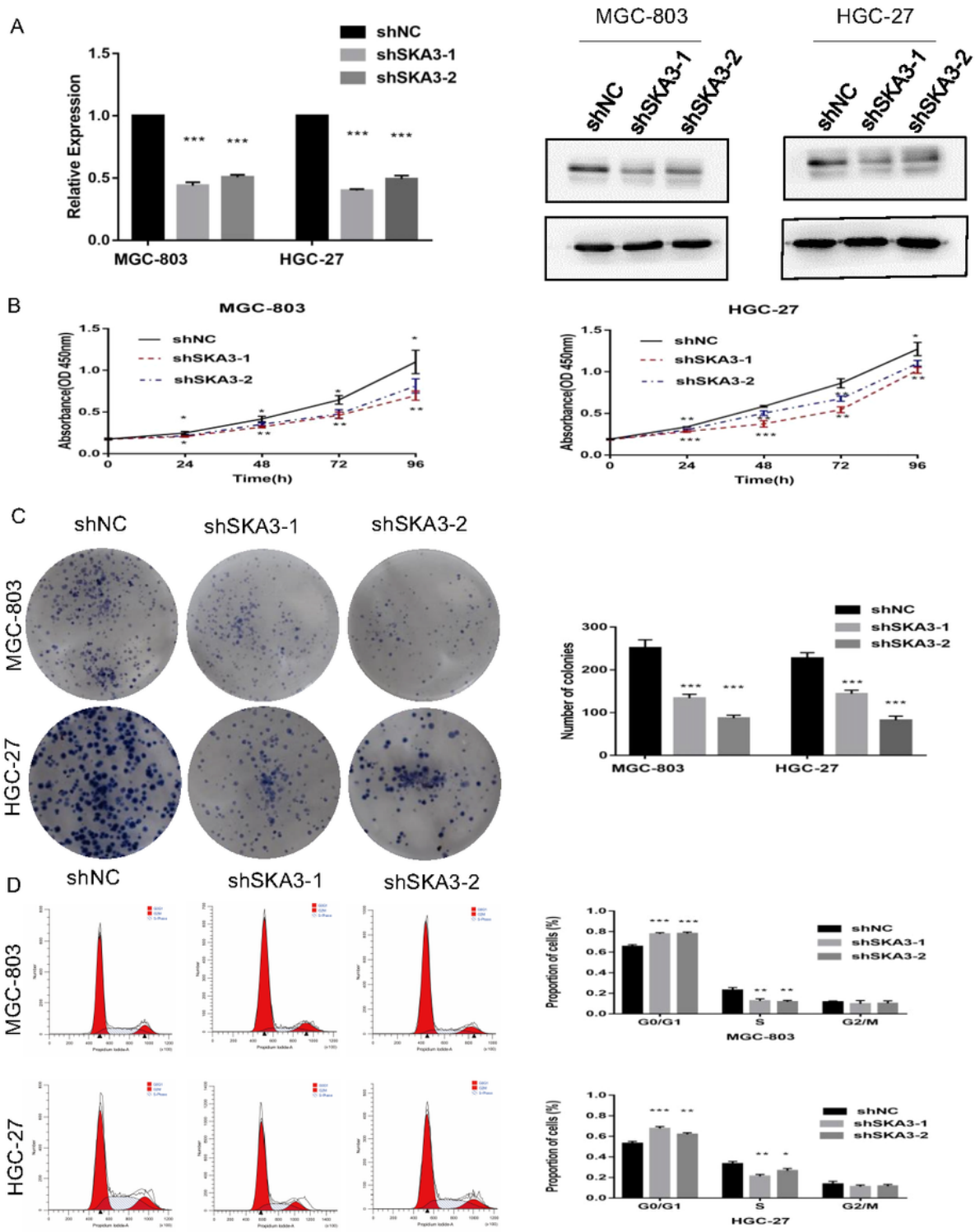

Figure 2

SKA3 promotes proliferation in gastric cancer. A mRNA and protein levels of SKA3 after transfection with shSKA3 lentivirus in MGC-803 and HGC-27. B CCK-8 cell proliferation assay detects cell viability by silenced for SKA3 in MGC-803 and HGC-27. C Cloning experiment detects cell growth by silenced for SKA3 in MGC-803 and HGC-27. D Flow cytometry detects cell cycle n by silenced for SKA3 in MGC-803

and HGC-27. Data are shown as mean ± SD for triplicate experiments. The two-tailed Student's unpaired t-test was used. *P < 0.05, **P < 0.01, ***P < 0.001

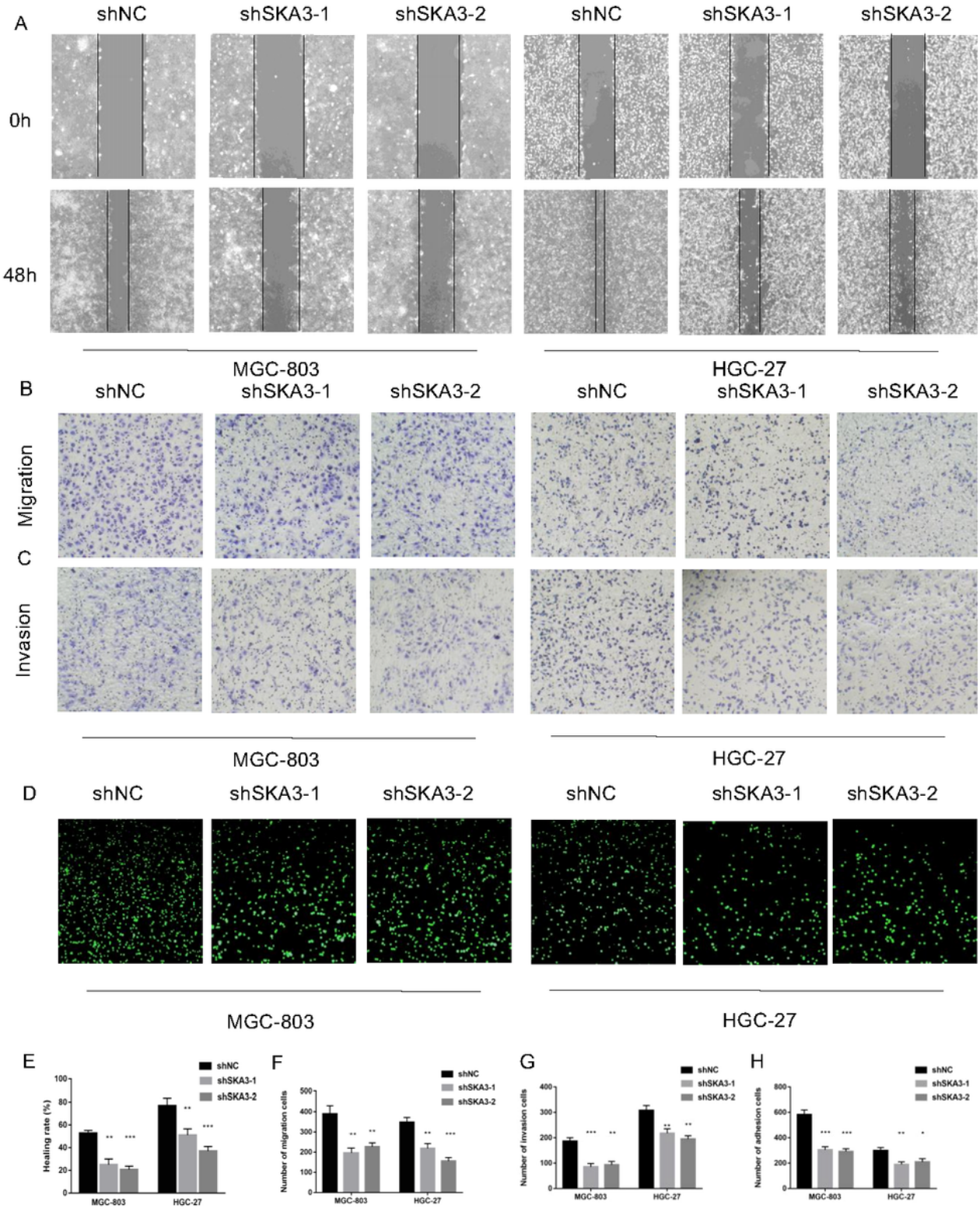

Figure 3

SKA3 promotes migration, invasion and adhesion in gastric cancer. A Wound-healing experiments detects cell migration by silenced for SKA3 in MGC-803 and HGC-27. B Transwell experiment detects cell migration by silenced for SKA3 in MGC-803 and HGC-27. C Transwell experiment detects cell invasion by

silenced for SKA3 in MGC-803 and HGC-27. D Adhesion experiment detects cell adhesion by silenced for SKA3 in MGC-803 and HGC-27. E Relative healing rate in (A) were quantified and shown. F Relative migration numbers in (B) were quantified and shown. G Relative invasion numbers in (C) were quantified and shown. H Relative adhesion numbers in (D) were quantified and shown. Data are shown as mean ± SD for triplicate experiments. The two-tailed Student's unpaired t-test was used. **P < 0.01, ***P < 0.001

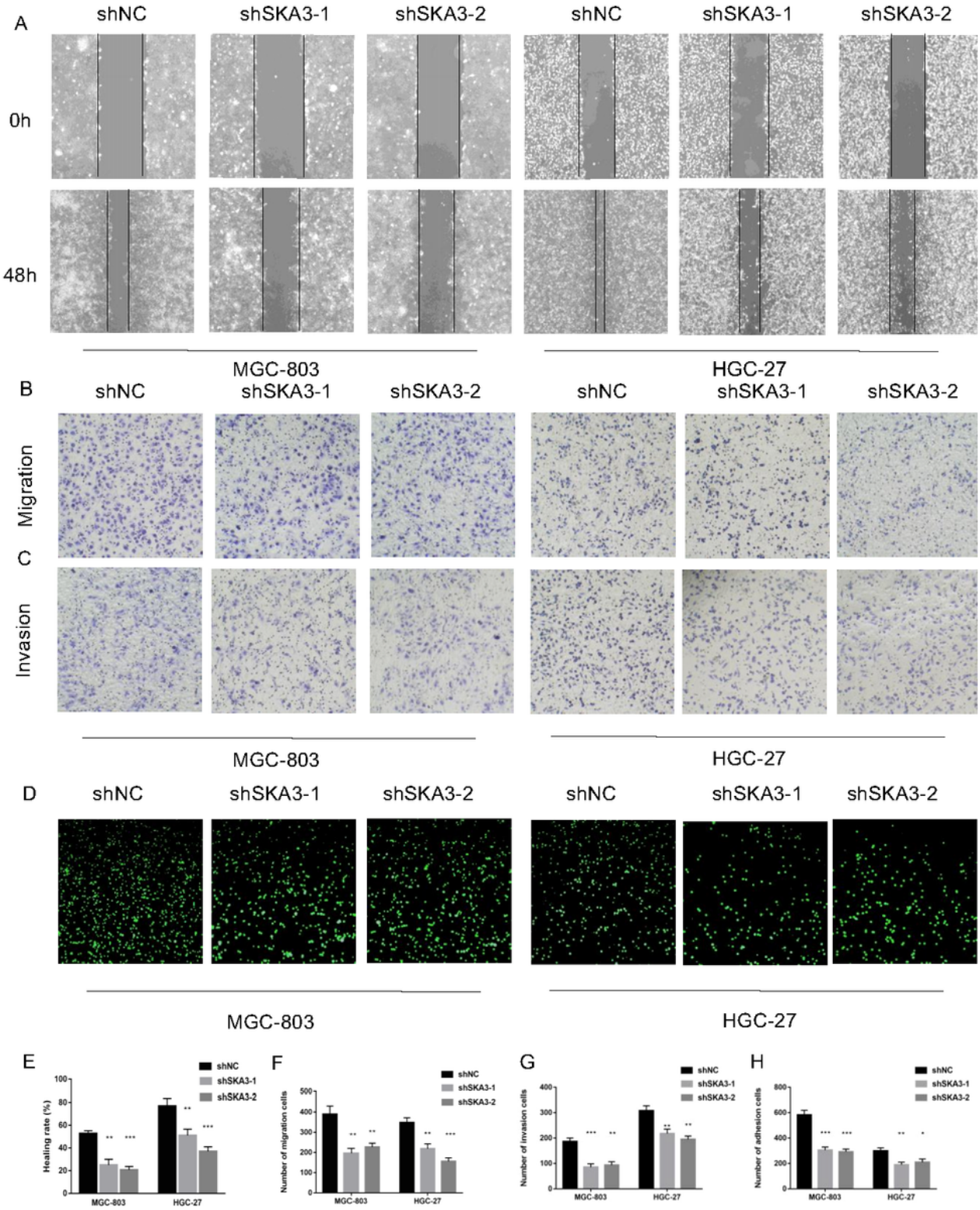

Figure 3

SKA3 promotes migration, invasion and adhesion in gastric cancer. A Wound-healing experiments detects cell migration by silenced for SKA3 in MGC-803 and HGC-27. B Transwell experiment detects cell migration by silenced for SKA3 in MGC-803 and HGC-27. C Transwell experiment detects cell invasion by silenced for SKA3 in MGC-803 and HGC-27. D Adhesion experiment detects cell adhesion by silenced for SKA3 in MGC-803 and HGC-27. E Relative healing rate in (A) were quantified and shown. F Relative migration numbers in (B) were quantified and shown. G Relative invasion numbers in (C) were quantified and shown. H Relative adhesion numbers in (D) were quantified and shown. Data are shown as mean ± SD for triplicate experiments. The two-tailed Student's unpaired t-test was used. **P < 0.01, ***P < 0.001

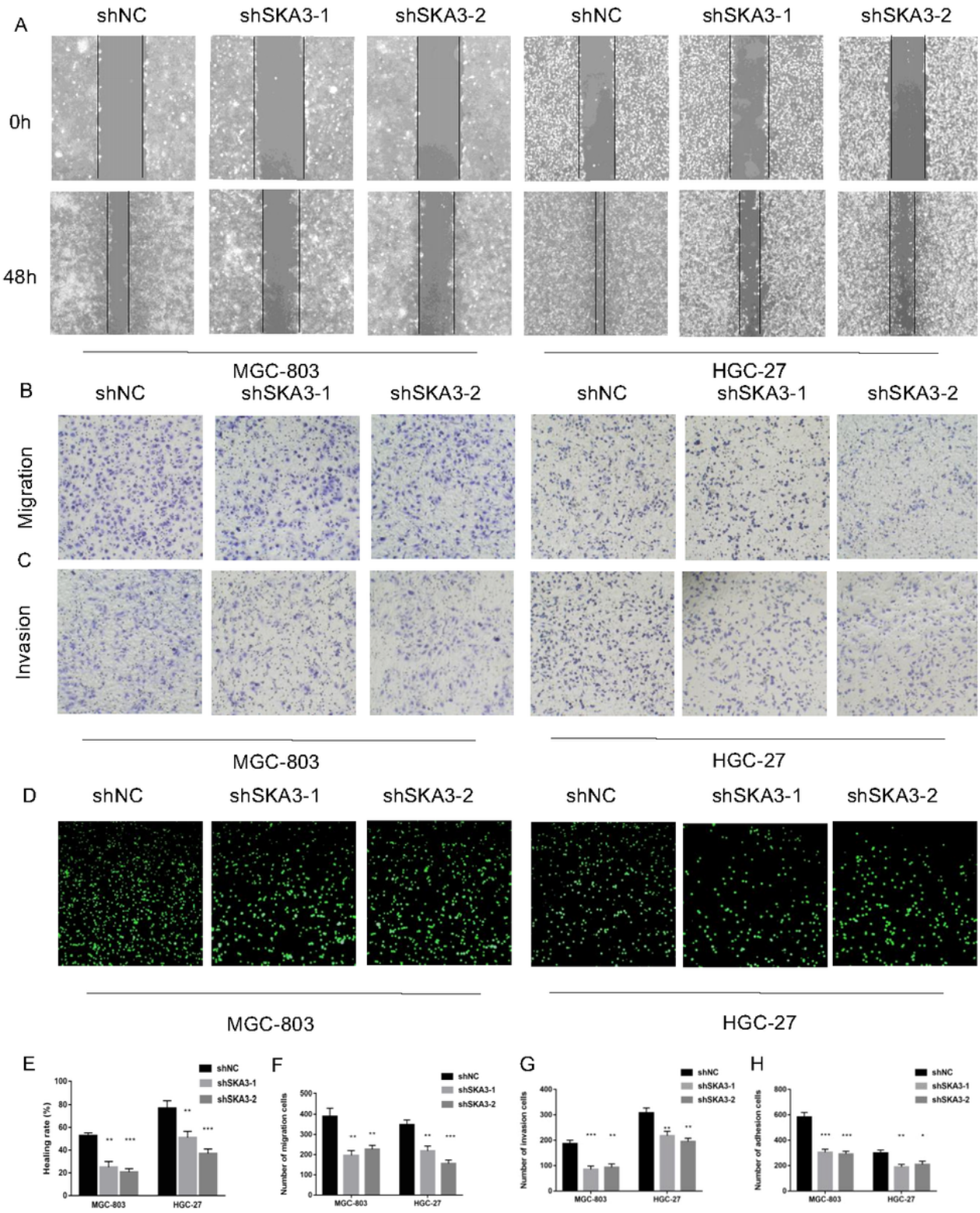

Figure 3

SKA3 promotes migration, invasion and adhesion in gastric cancer. A Wound-healing experiments detects cell migration by silenced for SKA3 in MGC-803 and HGC-27. B Transwell experiment detects cell migration by silenced for SKA3 in MGC-803 and HGC-27. C Transwell experiment detects cell invasion by silenced for SKA3 in MGC-803 and HGC-27. D Adhesion experiment detects cell adhesion by silenced for SKA3 in MGC-803 and HGC-27. E Relative healing rate in (A) were quantified and shown. F Relative

migration numbers in (B) were quantified and shown. G Relative invasion numbers in (C) were quantified and shown. H Relative adhesion numbers in (D) were quantified and shown. Data are shown as mean ± SD for triplicate experiments. The two-tailed Student's unpaired t-test was used. **P < 0.01, ***P < 0.001

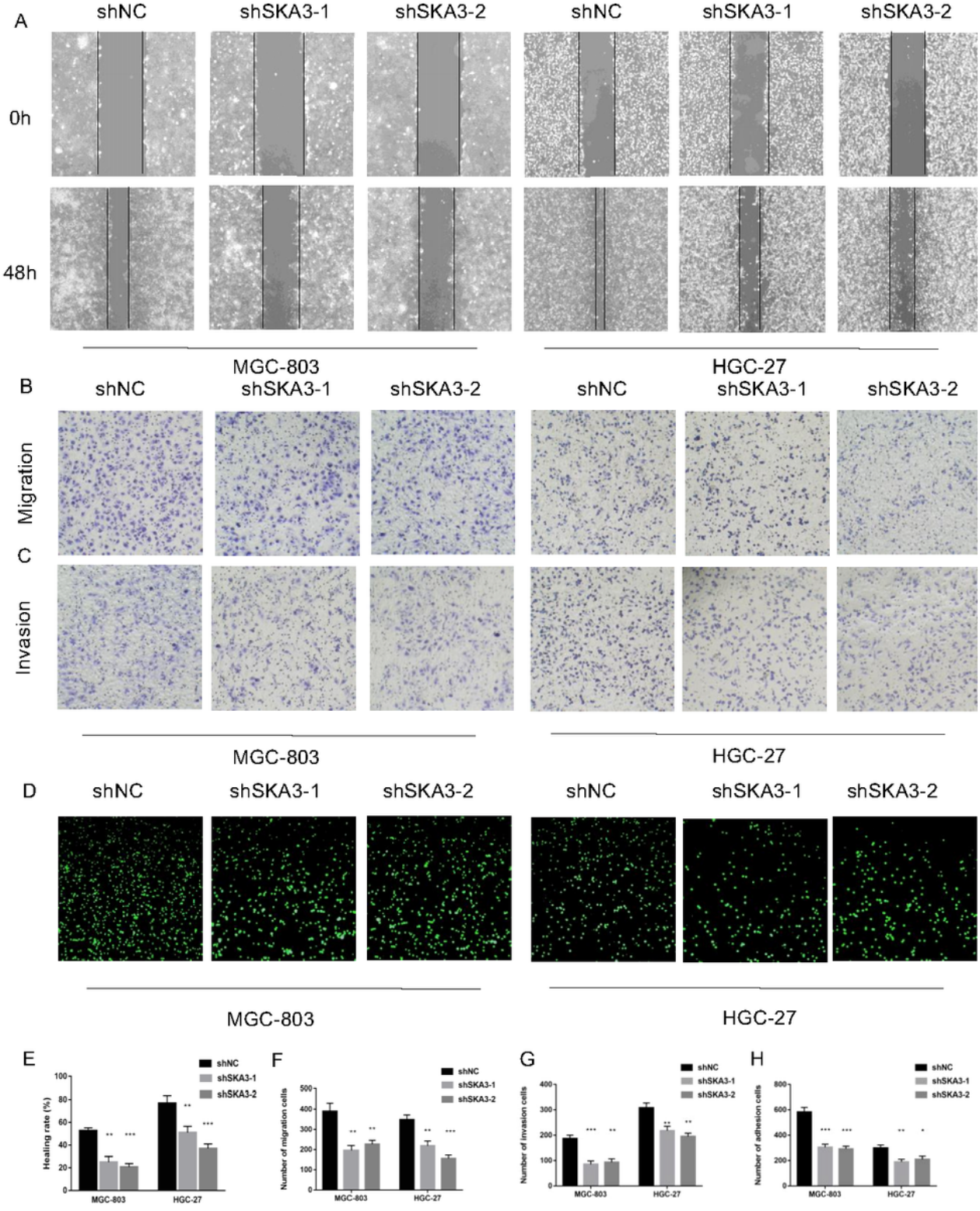

Figure 3

SKA3 promotes migration, invasion and adhesion in gastric cancer. A Wound-healing experiments detects cell migration by silenced for SKA3 in MGC-803 and HGC-27. B Transwell experiment detects cell

migration by silenced for SKA3 in MGC-803 and HGC-27. C Transwell experiment detects cell invasion by silenced for SKA3 in MGC-803 and HGC-27. D Adhesion experiment detects cell adhesion by silenced for SKA3 in MGC-803 and HGC-27. E Relative healing rate in (A) were quantified and shown. F Relative migration numbers in (B) were quantified and shown. G Relative invasion numbers in (C) were quantified and shown. H Relative adhesion numbers in (D) were quantified and shown. Data are shown as mean ± SD for triplicate experiments. The two-tailed Student's unpaired t-test was used. **P < 0.01, ***P < 0.001

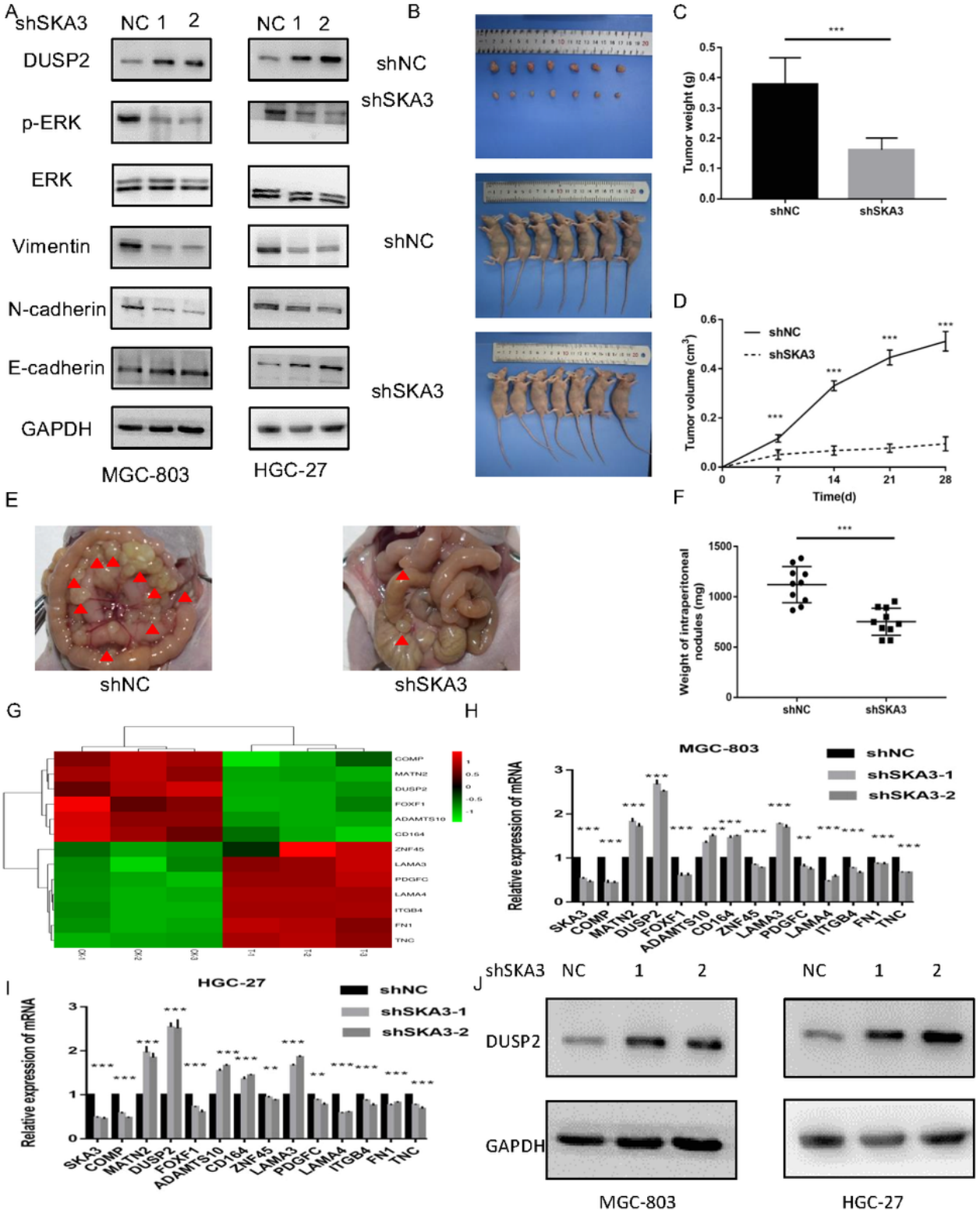

Figure 4

SKA3 regulates epithelial-mesenchymal transition (EMT), MAPK/ERK pathway in vitro and regulates the aggressive behaviors in vivo. A Silenced for SKA3 inhibits EMT and MAPK/ERK related proteins in MGC-803 and HGC-27. B Tumor growth assessment in subcutaneous tumor model of gastric cancer. C Tumor weight was measured in shSKA3 and control groups. D Tumor volume was measured in shSKA3 and control groups. E Intraperitoneal metastasis model showed that the metastatic nodules derived from shSKA3 and control groups. F Intraperitoneal metastasis tumor weight was measured in shSKA3 and control groups. G Microarray heatmap showed differentially expressed genes. H Differentially expressed genes were screened by qRT-PCR in MGC-803. I Differentially expressed genes were screened by qRT-PCR in HGC-27. J Western blot of DUSP2 levels in the sh-SKA3 cells. Data are shown as mean ± SD for triplicate experiments. The two-tailed Student's unpaired t-test was used. *P < 0.05, **P < 0.01, ***P < 0.001

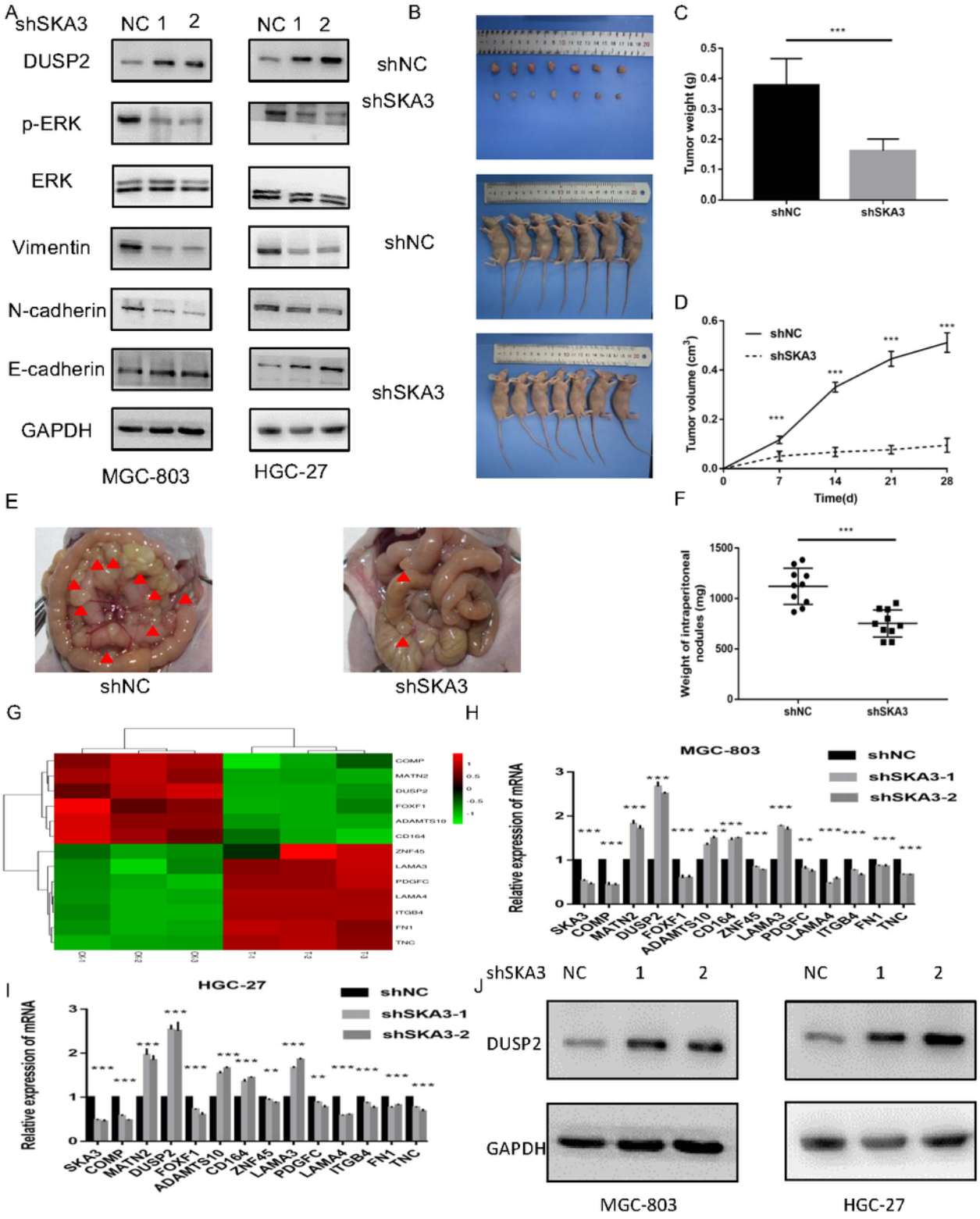

Figure 4

SKA3 regulates epithelial-mesenchymal transition (EMT), MAPK/ERK pathway in vitro and regulates the aggressive behaviors in vivo. A Silenced for SKA3 inhibits EMT and MAPK/ERK related proteins in MGC-803 and HGC-27. B Tumor growth assessment in subcutaneous tumor model of gastric cancer. C Tumor weight was measured in shSKA3 and control groups. D Tumor volume was measured in shSKA3 and control groups. E Intraperitoneal metastasis model showed that the metastatic nodules derived from

shSKA3 and control groups. F Intraperitoneal metastasis tumor weight was measured in shSKA3 and control groups. G Microarray heatmap showed differentially expressed genes. H Differentially expressed genes were screened by qRT-PCR in MGC-803. I Differentially expressed genes were screened by qRT-PCR in HGC-27. J Western blot of DUSP2 levels in the sh-SKA3 cells. Data are shown as mean ± SD for triplicate experiments. The two-tailed Student's unpaired t-test was used. *P < 0.05, **P < 0.01, ***P < 0.001

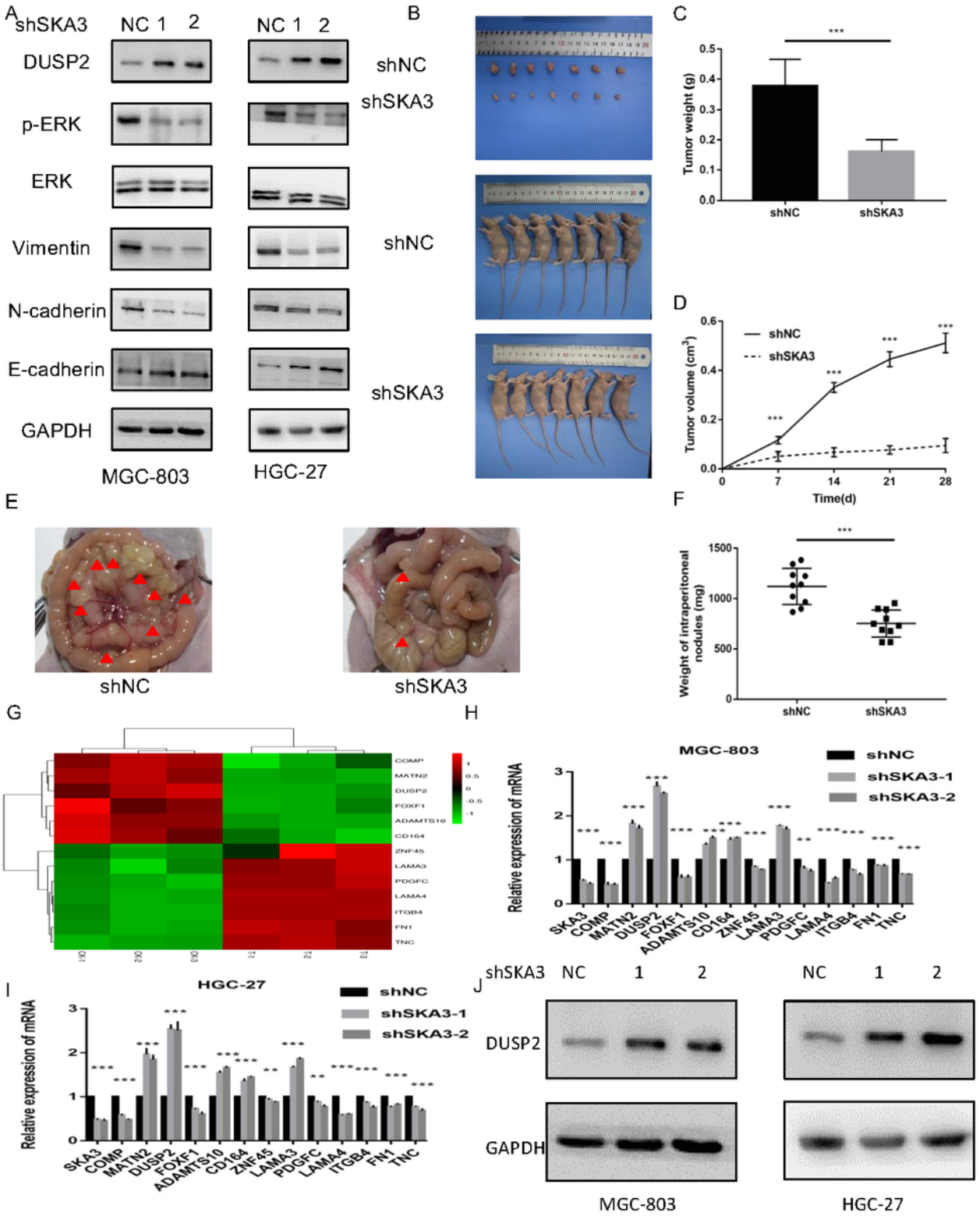

Figure 4

SKA3 regulates epithelial-mesenchymal transition (EMT), MAPK/ERK pathway in vitro and regulates the aggressive behaviors in vivo. A Silenced for SKA3 inhibits EMT and MAPK/ERK related proteins in MGC-803 and HGC-27. B Tumor growth assessment in subcutaneous tumor model of gastric cancer. C Tumor weight was measured in shSKA3 and control groups. D Tumor volume was measured in shSKA3 and control groups. E Intraperitoneal metastasis model showed that the metastatic nodules derived from shSKA3 and control groups. F Intraperitoneal metastasis tumor weight was measured in shSKA3 and control groups. G Microarray heatmap showed differentially expressed genes. H Differentially expressed genes were screened by qRT-PCR in MGC-803. I Differentially expressed genes were screened by qRT-PCR in HGC-27. J Western blot of DUSP2 levels in the sh-SKA3 cells. Data are shown as mean ± SD for triplicate experiments. The two-tailed Student's unpaired t-test was used. *P < 0.05, **P < 0.01, ***P < 0.001

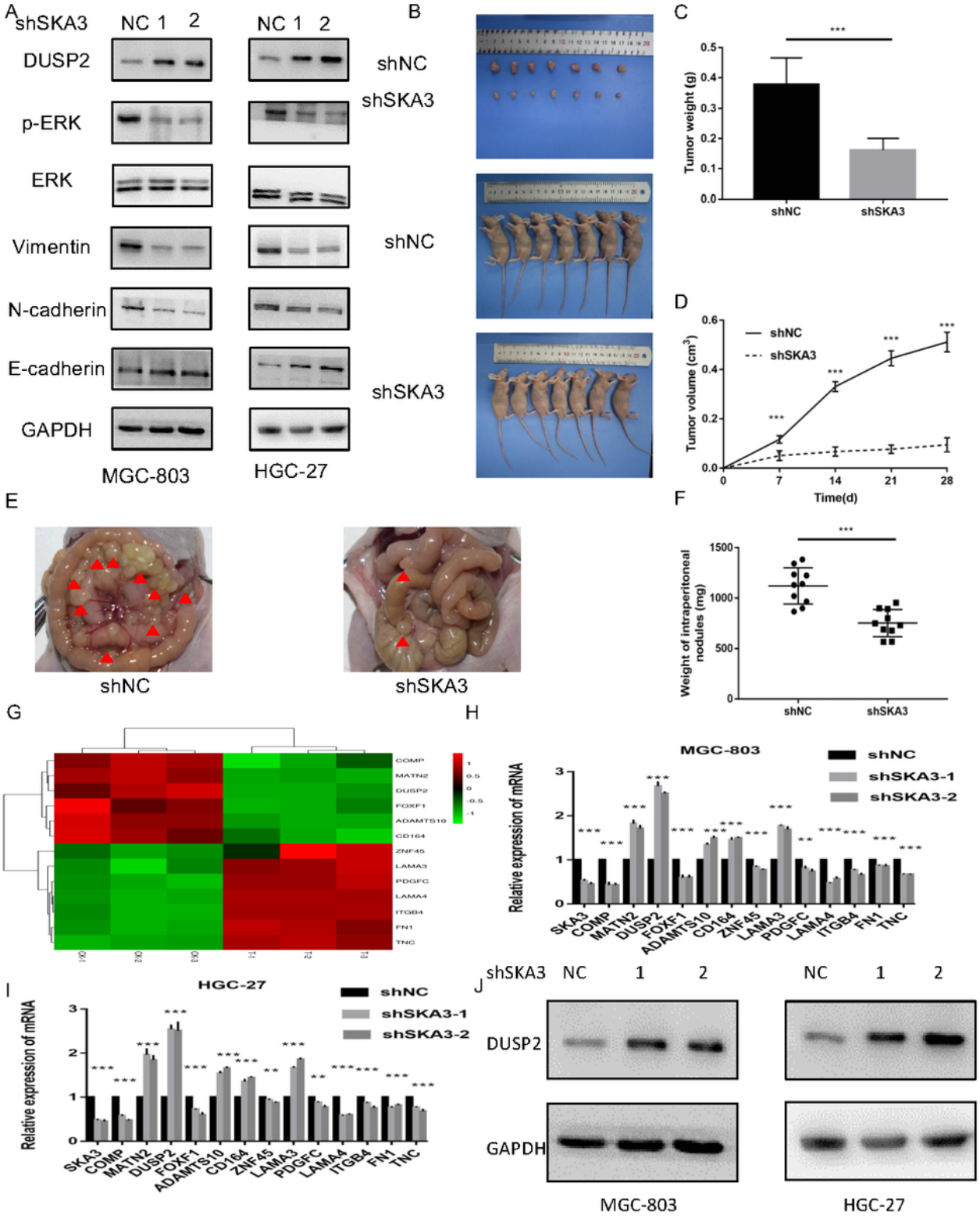

Figure 4

SKA3 regulates epithelial-mesenchymal transition (EMT), MAPK/ERK pathway in vitro and regulates the aggressive behaviors in vivo. A Silenced for SKA3 inhibits EMT and MAPK/ERK related proteins in MGC-803 and HGC-27. B Tumor growth assessment in subcutaneous tumor model of gastric cancer. C Tumor weight was measured in shSKA3 and control groups. D Tumor volume was measured in shSKA3 and control groups. E Intraperitoneal metastasis model showed that the metastatic nodules derived from

shSKA3 and control groups. F Intraperitoneal metastasis tumor weight was measured in shSKA3 and control groups. G Microarray heatmap showed differentially expressed genes. H Differentially expressed genes were screened by qRT-PCR in MGC-803. I Differentially expressed genes were screened by qRT-PCR in HGC-27. J Western blot of DUSP2 levels in the sh-SKA3 cells. Data are shown as mean ± SD for triplicate experiments. The two-tailed Student's unpaired t-test was used. *P < 0.05, **P < 0.01, ***P < 0.001

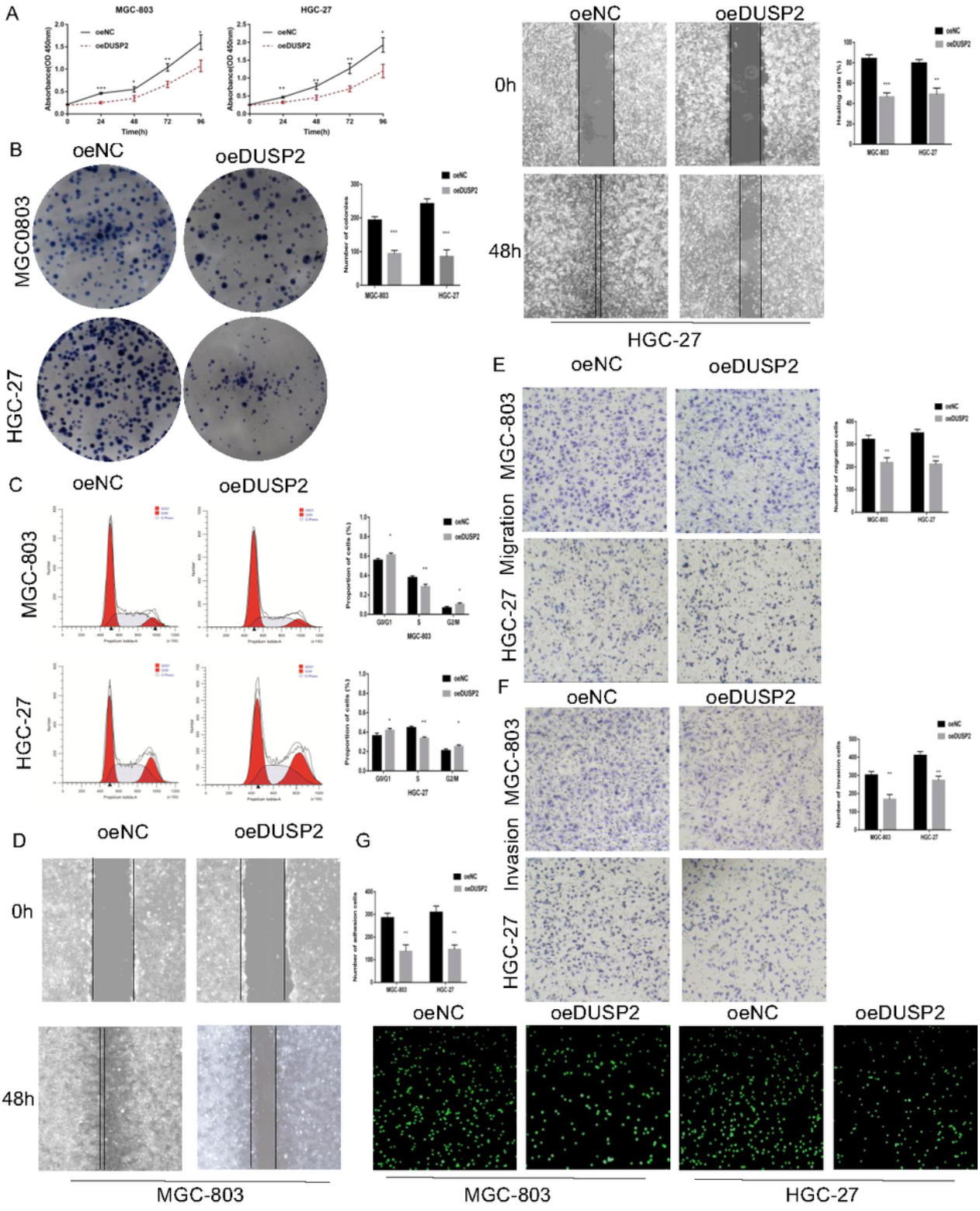

Figure 5

DUSP2 inhibits proliferation, migration, invasion and adhesion in gastric cancer. A CCK-8 cell proliferation assay detects cell viability by overexpression for DUSP2 in MGC-803 and HGC-27. B Cloning experiment detects cell growth by overexpression for DUSP2 in MGC-803 and HGC-27. C Flow cytometry detects cell cycle by overexpression for DUSP2 in MGC-803 and HGC-27. D Wound-healing experiments detects cell migration by overexpression for DUSP2 in MGC-803 and HGC-27. E Transwell experiment detects cell migration by overexpression for SKA3 in MGC-803. F Transwell experiment detects cell migration by overexpression for SKA3 in HGC-27. G Adhesion experiment detects cell adhesion by overexpression for SKA3 in MGC-803 and HGC-27. Data are shown as mean ± SD for triplicate experiments. The two-tailed Student's unpaired t-test was used. *P < 0.05, **P < 0.01, ***P < 0.001

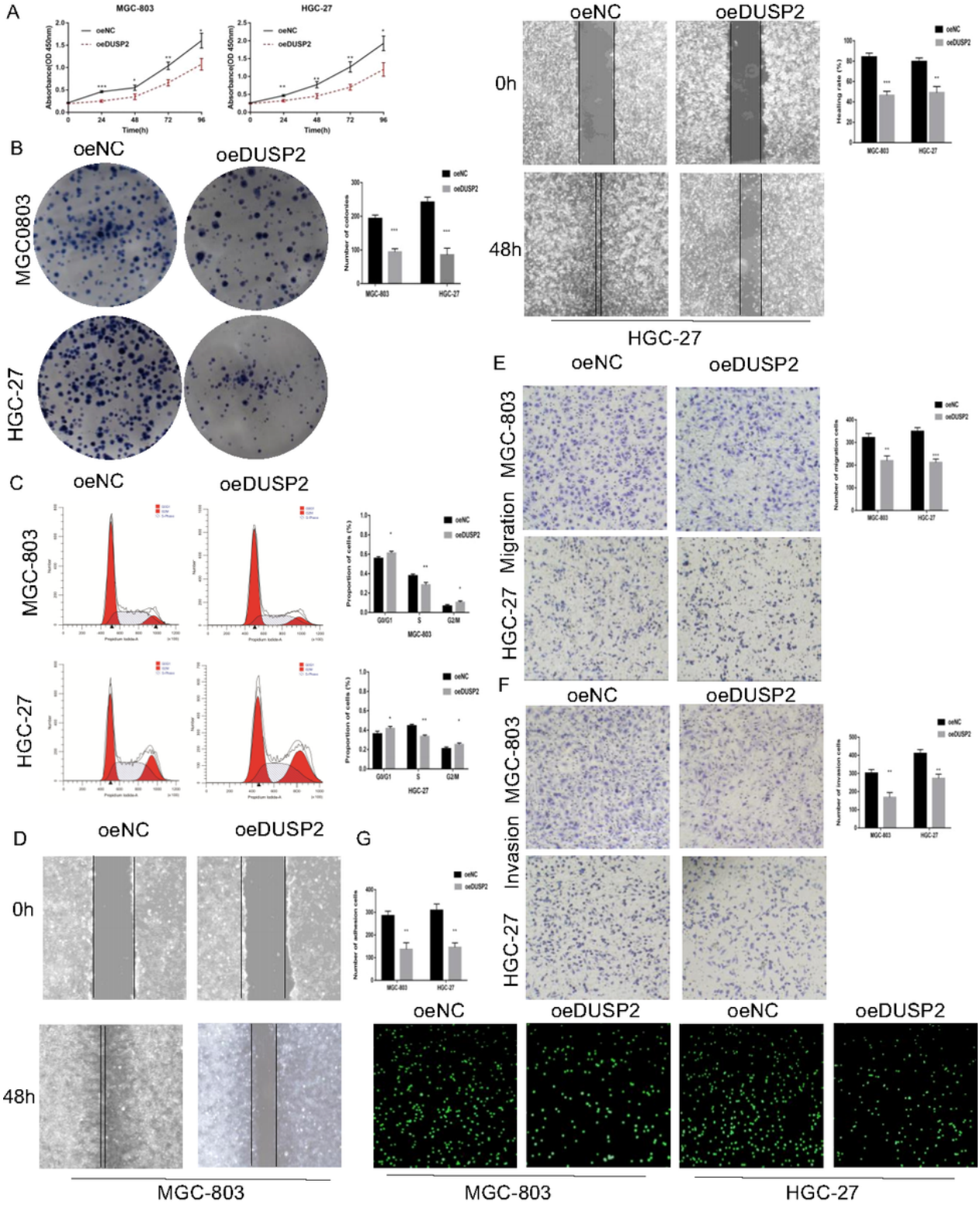

Figure 5

DUSP2 inhibits proliferation, migration, invasion and adhesion in gastric cancer. A CCK-8 cell proliferation assay detects cell viability by overexpression for DUSP2 in MGC-803 and HGC-27. B Cloning experiment detects cell growth by overexpression for DUSP2 in MGC-803 and HGC-27. C Flow cytometry detects cell cycle by overexpression for DUSP2 in MGC-803 and HGC-27. D Wound-healing experiments detects cell migration by overexpression for DUSP2 in MGC-803 and HGC-27. E Transwell experiment detects cell

migration by overexpression for SKA3 in MGC-803. F Transwell experiment detects cell migration by overexpression for SKA3 in HGC-27. G Adhesion experiment detects cell adhesion by overexpression for SKA3 in MGC-803 and HGC-27. Data are shown as mean ± SD for triplicate experiments. The two-tailed Student's unpaired t-test was used. *P < 0.05, **P < 0.01, ***P < 0.001

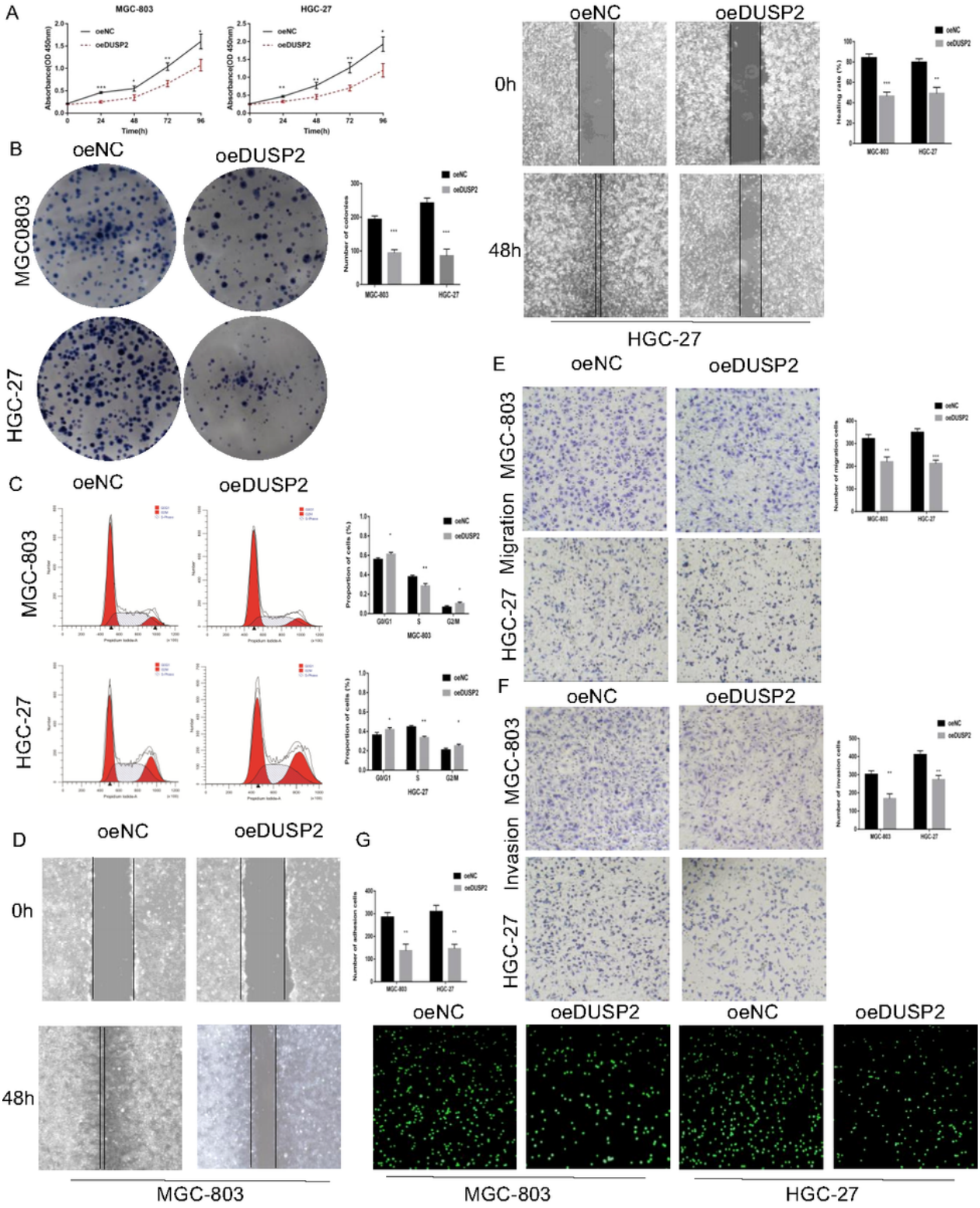

Figure 5

DUSP2 inhibits proliferation, migration, invasion and adhesion in gastric cancer. A CCK-8 cell proliferation assay detects cell viability by overexpression for DUSP2 in MGC-803 and HGC-27. B Cloning experiment detects cell growth by overexpression for DUSP2 in MGC-803 and HGC-27. C Flow cytometry detects cell cycle by overexpression for DUSP2 in MGC-803 and HGC-27. D Wound-healing experiments detects cell migration by overexpression for DUSP2 in MGC-803 and HGC-27. E Transwell experiment detects cell migration by overexpression for SKA3 in MGC-803. F Transwell experiment detects cell migration by overexpression for SKA3 in HGC-27. G Adhesion experiment detects cell adhesion by overexpression for SKA3 in MGC-803 and HGC-27. Data are shown as mean ± SD for triplicate experiments. The two-tailed Student's unpaired t-test was used. *P < 0.05, **P < 0.01, ***P < 0.001

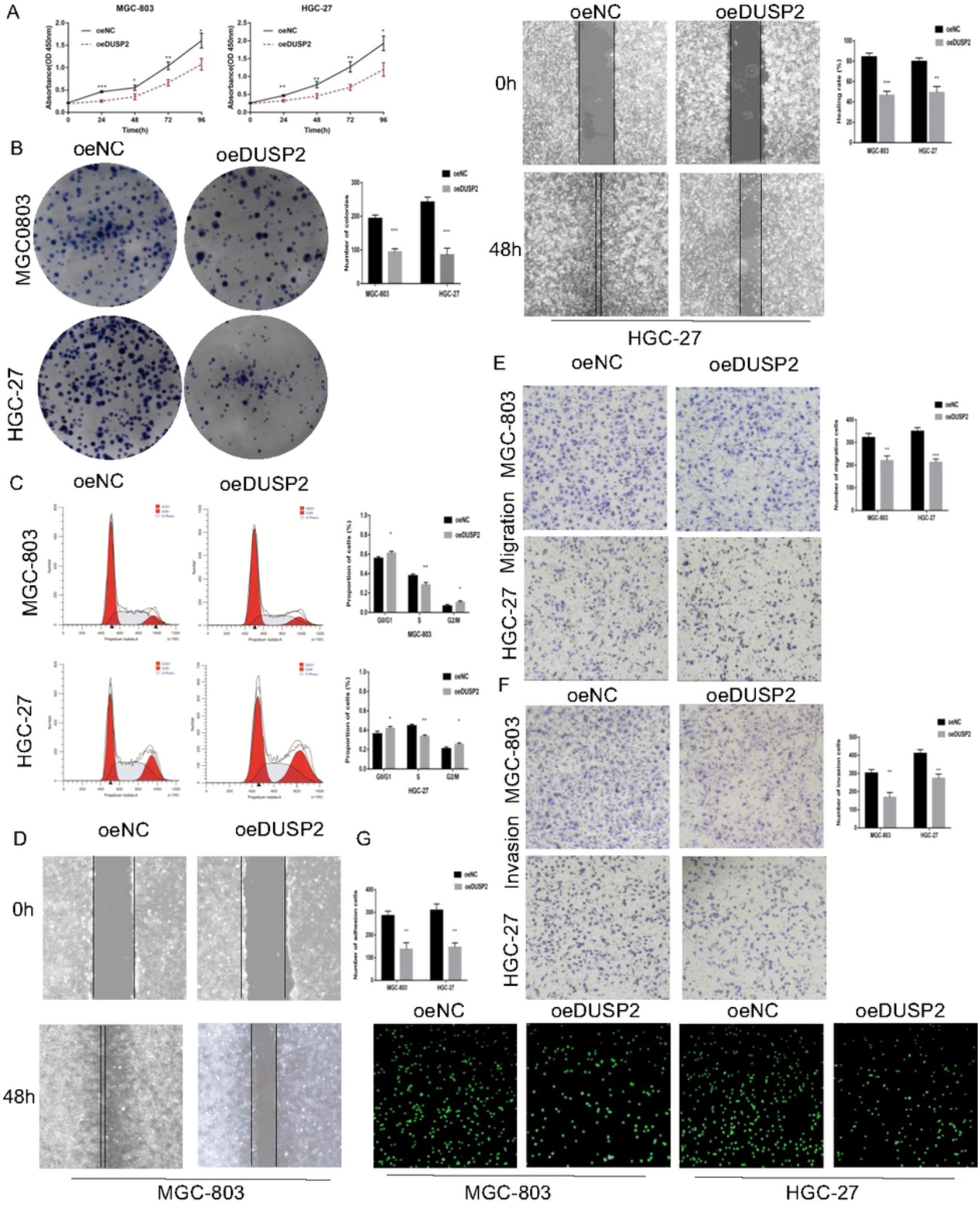

Figure 5

DUSP2 inhibits proliferation, migration, invasion and adhesion in gastric cancer. A CCK-8 cell proliferation assay detects cell viability by overexpression for DUSP2 in MGC-803 and HGC-27. B Cloning experiment detects cell growth by overexpression for DUSP2 in MGC-803 and HGC-27. C Flow cytometry detects cell cycle by overexpression for DUSP2 in MGC-803 and HGC-27. D Wound-healing experiments detects cell migration by overexpression for DUSP2 in MGC-803 and HGC-27. E Transwell experiment detects cell

migration by overexpression for SKA3 in MGC-803. F Transwell experiment detects cell migration by overexpression for SKA3 in HGC-27. G Adhesion experiment detects cell adhesion by overexpression for SKA3 in MGC-803 and HGC-27. Data are shown as mean ± SD for triplicate experiments. The two-tailed Student's unpaired t-test was used. *P < 0.05, **P < 0.01, ***P < 0.001

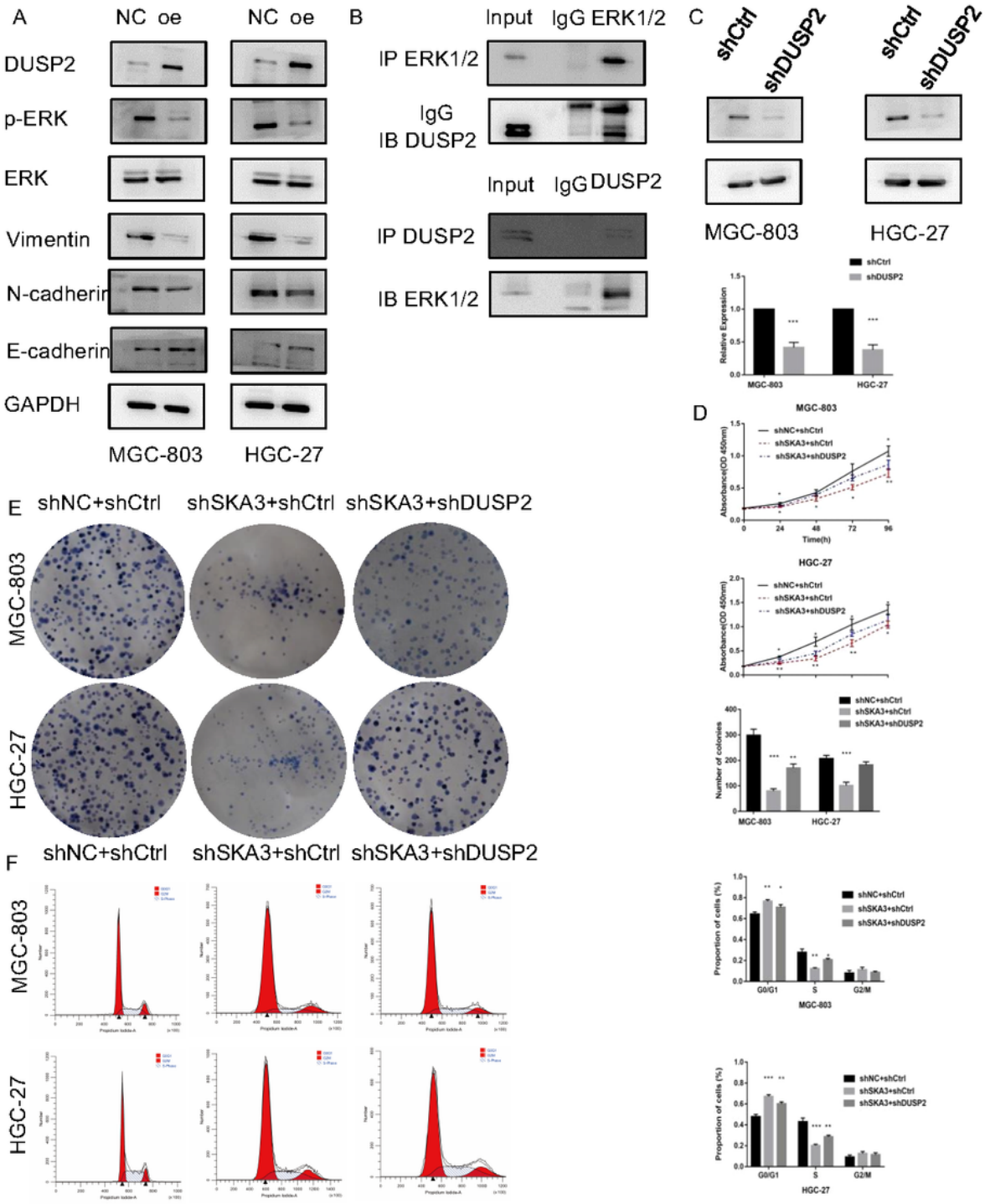

Figure 6

SKA3 mediates DUSP2 induced proliferation, EMT by inactivating MAPK/ERK pathway. A Overexpression for DUSP2 inhibits EMT and MAPK/ERK related proteins in MGC-803 and HGC-27. B HGC-27 cell total lysates were IP with the DUSP2 antibodies or ERK1/2 antibodies, followed by Western blotting using the indicated antibodies. C. mRNA and protein levels of DUSP2 after transfection with shDUSP2 lentivirus in MGC-803 and HGC-27. D The inhibiting effect of SKA3 downregulation on MGC-803 and HGC-27 CCK-8 cell proliferation was rescued by shDUSP2 transfection. E The inhibiting effect of SKA3 downregulation on MGC-803 and HGC-27 CCK-8 cell cloning was rescued by shDUSP2 transfection. F The inhibiting effect of SKA3 downregulation on MGC-803 and HGC-27 cell cycle was rescued by shDUSP2 transfection. Data are shown as mean ± SD for triplicate experiments. The two-tailed Student's unpaired t-test was used. *P < 0.05, **P < 0.01, ***P < 0.001

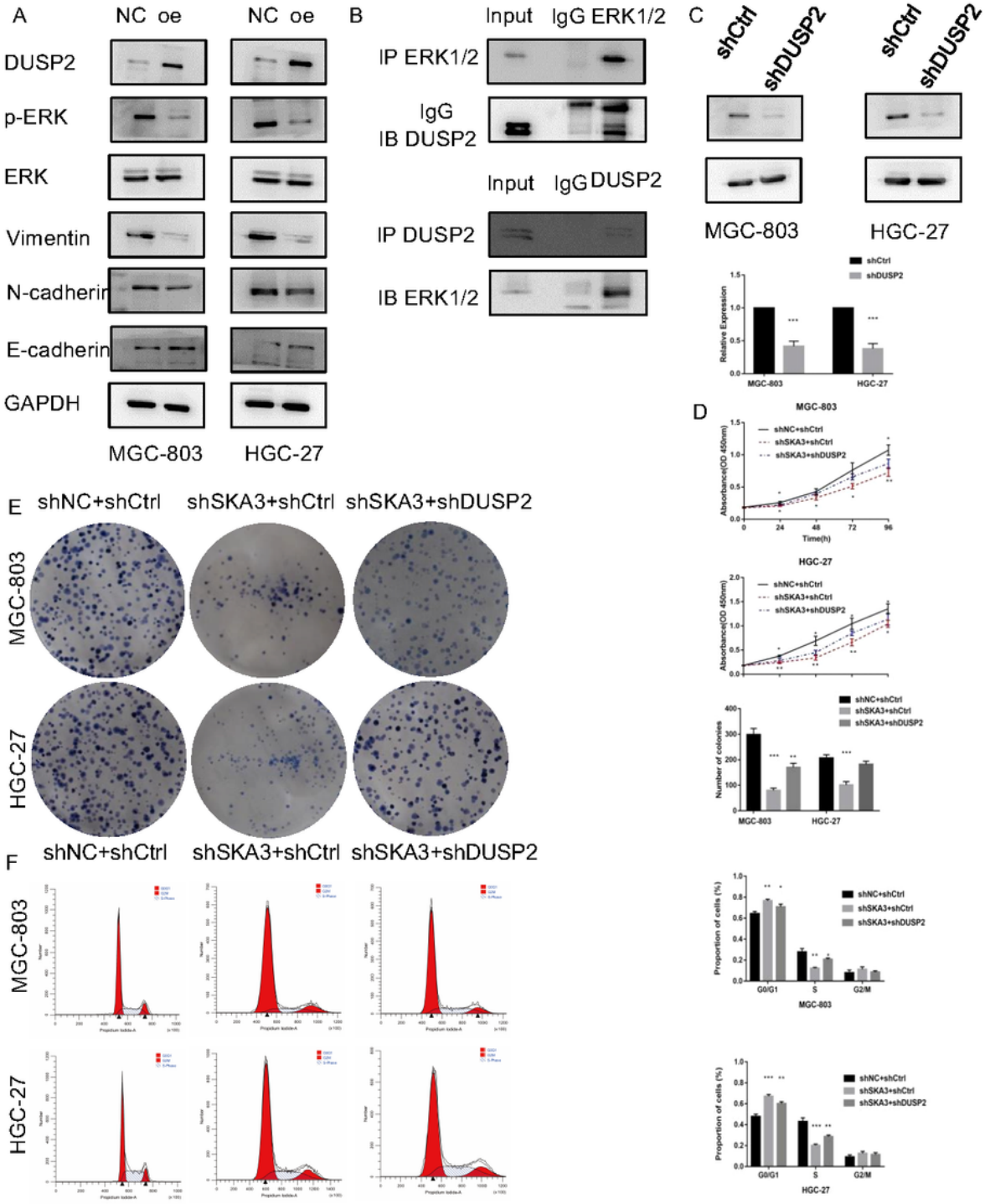

Figure 6

SKA3 mediates DUSP2 induced proliferation, EMT by inactivating MAPK/ERK pathway. A Overexpression for DUSP2 inhibits EMT and MAPK/ERK related proteins in MGC-803 and HGC-27. B HGC-27 cell total lysates were IP with the DUSP2 antibodies or ERK1/2 antibodies, followed by Western blotting using the indicated antibodies. C. mRNA and protein levels of DUSP2 after transfection with shDUSP2 lentivirus in MGC-803 and HGC-27. D The inhibiting effect of SKA3 downregulation on MGC-803 and HGC-27 CCK-8

cell proliferation was rescued by shDUSP2 transfection. E The inhibiting effect of SKA3 downregulation on MGC-803 and HGC-27 CCK-8 cell cloning was rescued by shDUSP2 transfection. F The inhibiting effect of SKA3 downregulation on MGC-803 and HGC-27 cell cycle was rescued by shDUSP2 transfection. Data are shown as mean ± SD for triplicate experiments. The two-tailed Student's unpaired t-test was used. *P < 0.05, **P < 0.01, ***P < 0.001

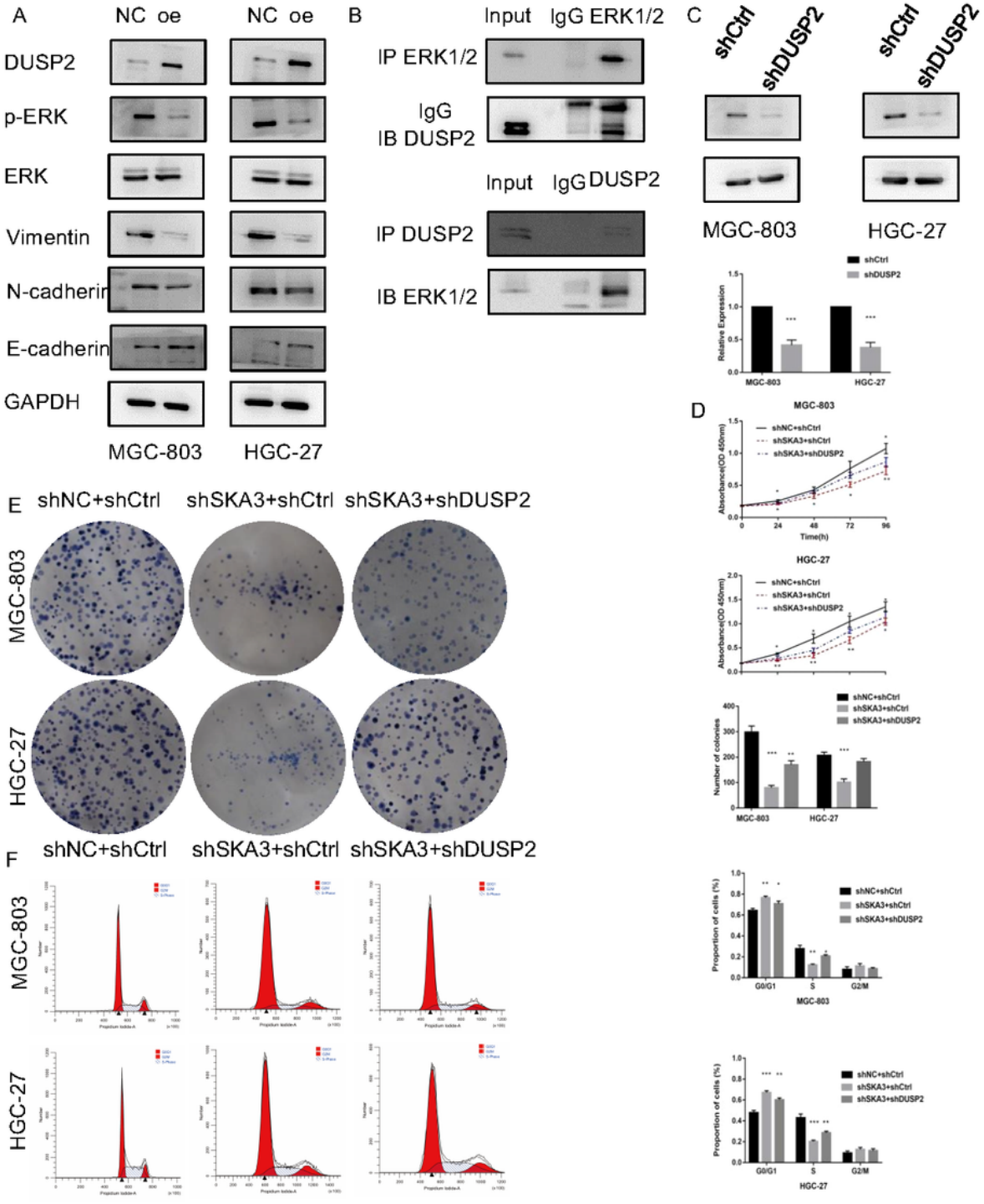

Figure 6

SKA3 mediates DUSP2 induced proliferation, EMT by inactivating MAPK/ERK pathway. A Overexpression for DUSP2 inhibits EMT and MAPK/ERK related proteins in MGC-803 and HGC-27. B HGC-27 cell total lysates were IP with the DUSP2 antibodies or ERK1/2 antibodies, followed by Western blotting using the indicated antibodies. C. mRNA and protein levels of DUSP2 after transfection with shDUSP2 lentivirus in MGC-803 and HGC-27. D The inhibiting effect of SKA3 downregulation on MGC-803 and HGC-27 CCK-8 cell proliferation was rescued by shDUSP2 transfection. E The inhibiting effect of SKA3 downregulation on MGC-803 and HGC-27 CCK-8 cell cloning was rescued by shDUSP2 transfection. F The inhibiting effect of SKA3 downregulation on MGC-803 and HGC-27 cell cycle was rescued by shDUSP2 transfection. Data are shown as mean ± SD for triplicate experiments. The two-tailed Student's unpaired t-test was used. *P < 0.05, **P < 0.01, ***P < 0.001

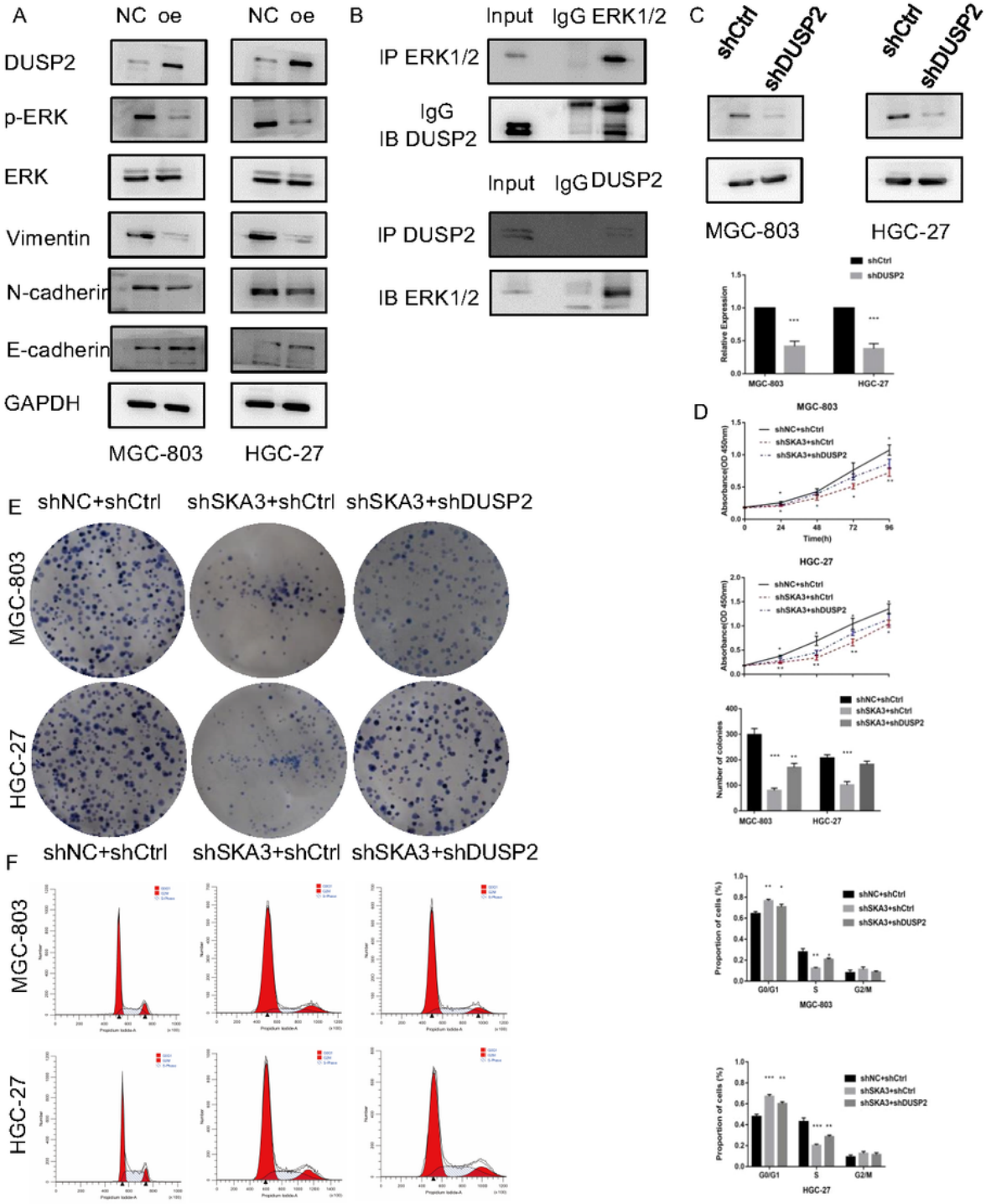

Figure 6

SKA3 mediates DUSP2 induced proliferation, EMT by inactivating MAPK/ERK pathway. A Overexpression for DUSP2 inhibits EMT and MAPK/ERK related proteins in MGC-803 and HGC-27. B HGC-27 cell total lysates were IP with the DUSP2 antibodies or ERK1/2 antibodies, followed by Western blotting using the indicated antibodies. C. mRNA and protein levels of DUSP2 after transfection with shDUSP2 lentivirus in MGC-803 and HGC-27. D The inhibiting effect of SKA3 downregulation on MGC-803 and HGC-27 CCK-8

cell proliferation was rescued by shDUSP2 transfection. E The inhibiting effect of SKA3 downregulation on MGC-803 and HGC-27 CCK-8 cell cloning was rescued by shDUSP2 transfection. F The inhibiting effect of SKA3 downregulation on MGC-803 and HGC-27 cell cycle was rescued by shDUSP2 transfection. Data are shown as mean ± SD for triplicate experiments. The two-tailed Student's unpaired t-test was used. *P < 0.05, **P < 0.01, ***P < 0.001

Figure 7

SKA3 mediates DUSP2 induced migration, invasion and adhesion by inactivating MAPK/ERK pathway. A The inhibiting effect of SKA3 downregulation on MGC-803 and HGC-27 wound-healing was rescued by shDUSP2 transfection. B The inhibiting effect of SKA3 downregulation on MGC-803 and HGC-27 migration was rescued by shDUSP2 transfection. C The inhibiting effect of SKA3 downregulation on MGC-803 and HGC-27 invasion was rescued by shDUSP2 transfection. D The inhibiting effect of SKA3 downregulation on MGC-803 and HGC-27 adhesion was rescued by shDUSP2 transfection. E Relative healing rate in (A) were quantified and shown. F Relative migration numbers in (B) were quantified and shown. G Relative invasion numbers in (C) were quantified and shown. H Relative adhesion numbers in (D) were quantified and shown. Data are shown as mean ± SD for triplicate experiments. The two-tailed Student's unpaired t-test was used. *P < 0.05, **P < 0.01, ***P < 0.001

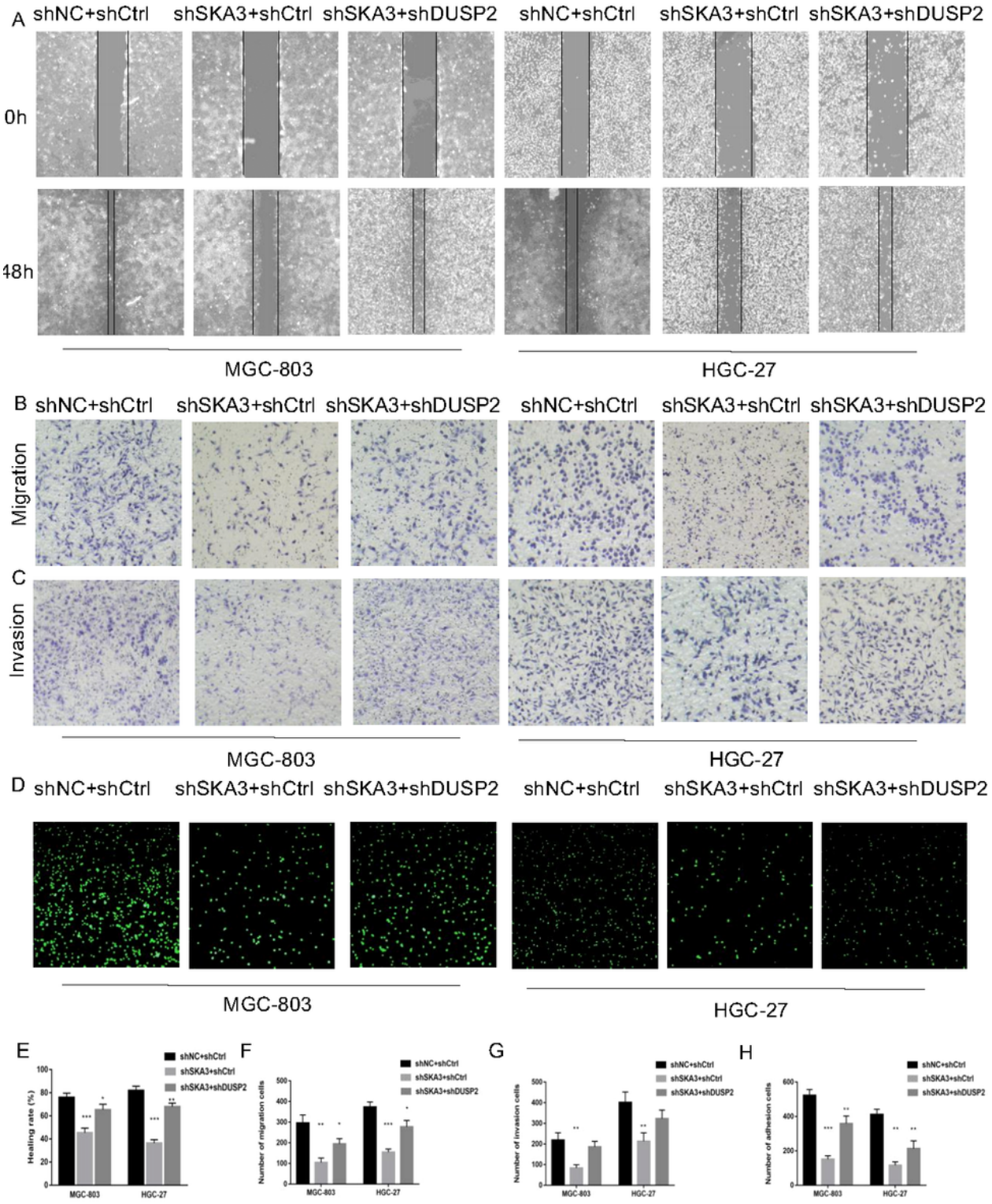

Figure 7

SKA3 mediates DUSP2 induced migration, invasion and adhesion by inactivating MAPK/ERK pathway. A The inhibiting effect of SKA3 downregulation on MGC-803 and HGC-27 wound-healing was rescued by shDUSP2 transfection. B The inhibiting effect of SKA3 downregulation on MGC-803 and HGC-27 migration was rescued by shDUSP2 transfection. C The inhibiting effect of SKA3 downregulation on MGC-803 and HGC-27 invasion was rescued by shDUSP2 transfection. D The inhibiting effect of SKA3

downregulation on MGC-803 and HGC-27 adhesion was rescued by shDUSP2 transfection. E Relative healing rate in (A) were quantified and shown. F Relative migration numbers in (B) were quantified and shown. G Relative invasion numbers in (C) were quantified and shown. H Relative adhesion numbers in (D) were quantified and shown. Data are shown as mean ± SD for triplicate experiments. The two-tailed Student's unpaired t-test was used. *P < 0.05, **P < 0.01, ***P < 0.001

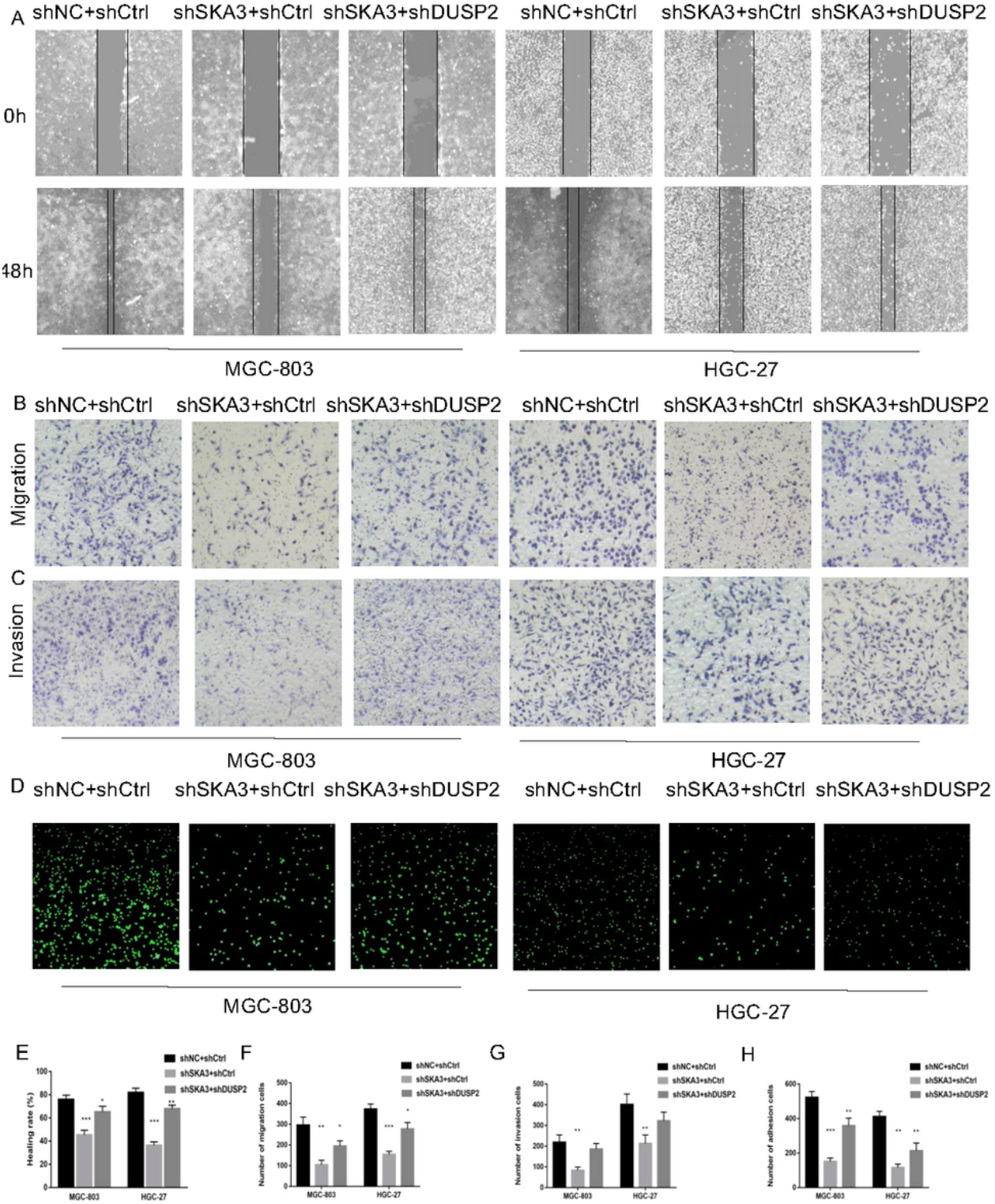

Figure 7

SKA3 mediates DUSP2 induced migration, invasion and adhesion by inactivating MAPK/ERK pathway. A The inhibiting effect of SKA3 downregulation on MGC-803 and HGC-27 wound-healing was rescued by shDUSP2 transfection. B The inhibiting effect of SKA3 downregulation on MGC-803 and HGC-27 migration was rescued by shDUSP2 transfection. C The inhibiting effect of SKA3 downregulation on MGC-803 and HGC-27 invasion was rescued by shDUSP2 transfection. D The inhibiting effect of SKA3 downregulation on MGC-803 and HGC-27 adhesion was rescued by shDUSP2 transfection. E Relative healing rate in (A) were quantified and shown. F Relative migration numbers in (B) were quantified and shown. G Relative invasion numbers in (C) were quantified and shown. H Relative adhesion numbers in (D) were quantified and shown. Data are shown as mean ± SD for triplicate experiments. The two-tailed Student's unpaired t-test was used. *P < 0.05, **P < 0.01, ***P < 0.001

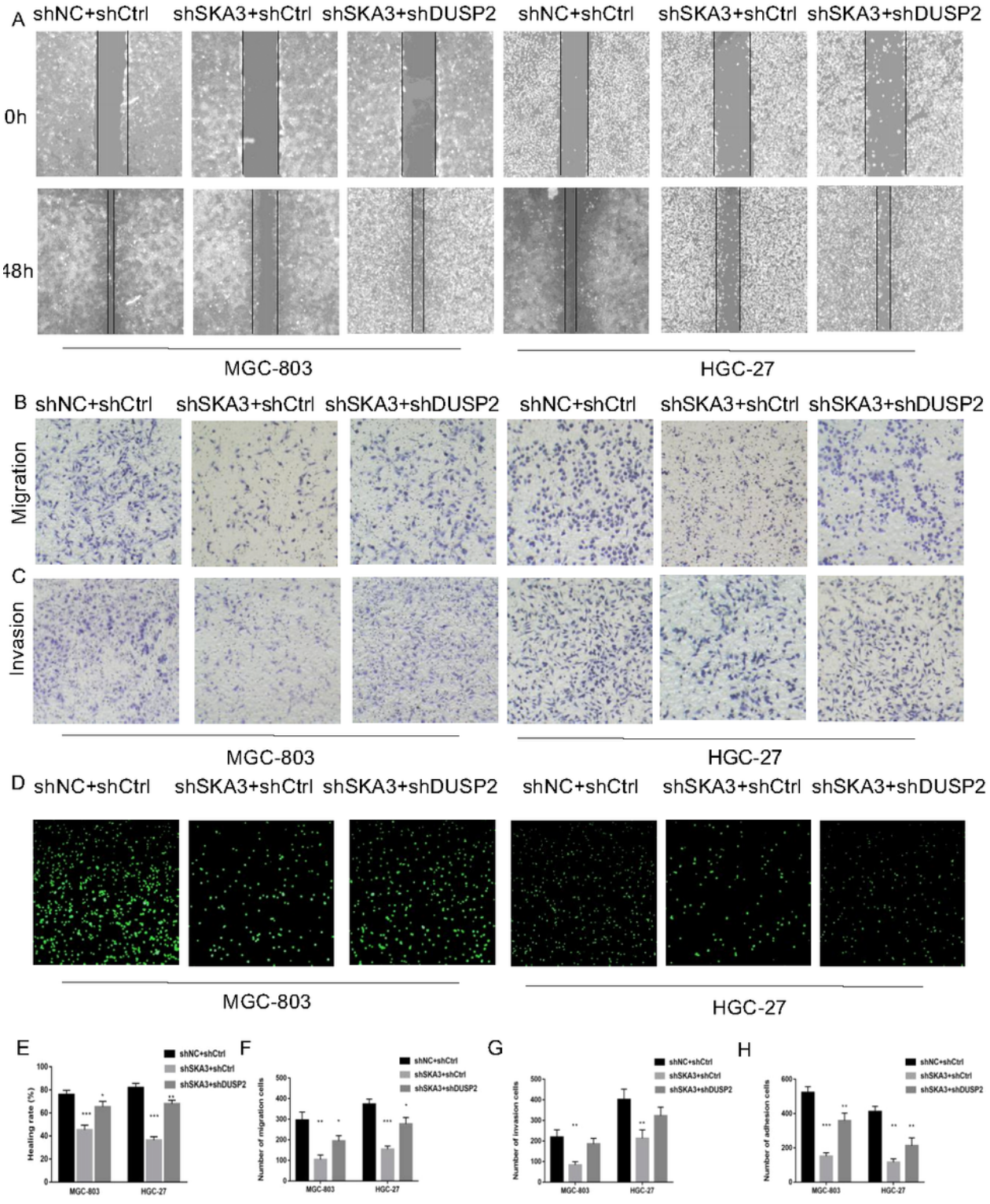

Figure 7

SKA3 mediates DUSP2 induced migration, invasion and adhesion by inactivating MAPK/ERK pathway. A The inhibiting effect of SKA3 downregulation on MGC-803 and HGC-27 wound-healing was rescued by shDUSP2 transfection. B The inhibiting effect of SKA3 downregulation on MGC-803 and HGC-27 migration was rescued by shDUSP2 transfection. C The inhibiting effect of SKA3 downregulation on MGC-803 and HGC-27 invasion was rescued by shDUSP2 transfection. D The inhibiting effect of SKA3

downregulation on MGC-803 and HGC-27 adhesion was rescued by shDUSP2 transfection. E Relative healing rate in (A) were quantified and shown. F Relative migration numbers in (B) were quantified and shown. G Relative invasion numbers in (C) were quantified and shown. H Relative adhesion numbers in (D) were quantified and shown. Data are shown as mean ± SD for triplicate experiments. The two-tailed Student's unpaired t-test was used. *P < 0.05, **P < 0.01, ***P < 0.001

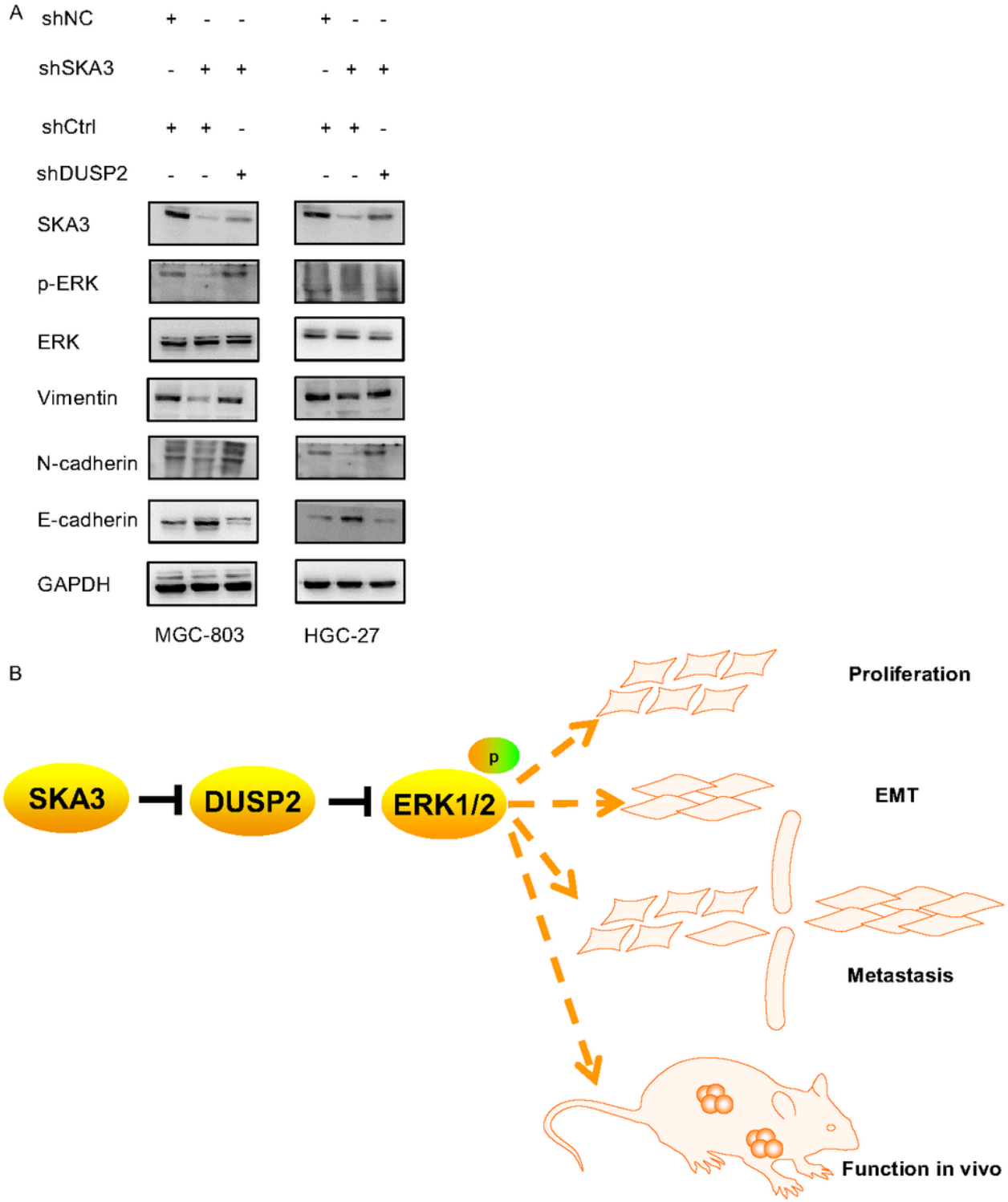

Figure 8

model illustrating SKA3-DUSP2-ERK1/2 axis in gastric cancer. A Co-transfected with shSKA3 and shDUSP2 rescue EMT and MAPK/ERK related proteins compared with shSKA3 group in MGC-803 and HGC-27. B Model of SKA3-DUSP2-ERK1/2 axis in gastric cancer

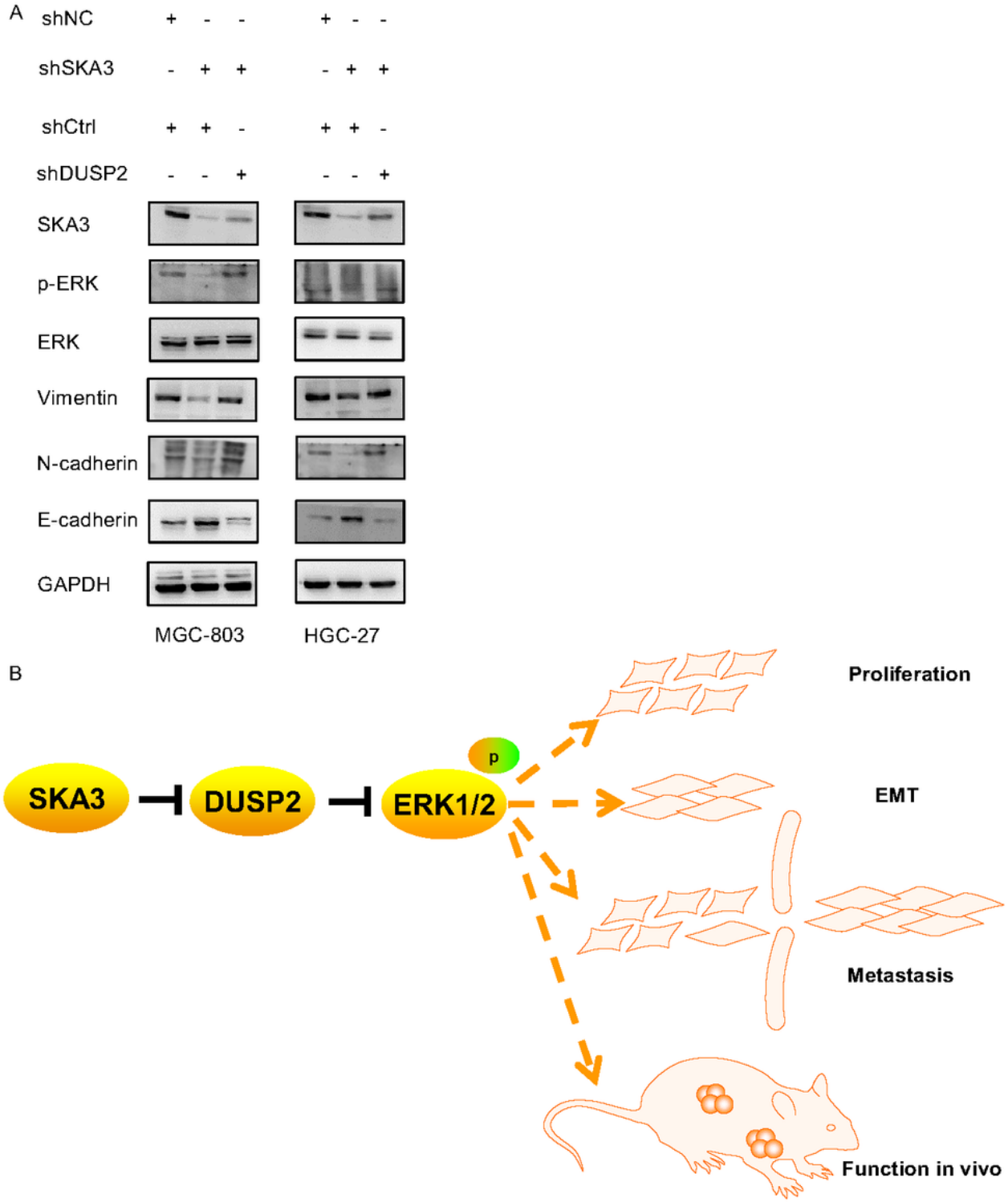

Figure 8

model illustrating SKA3-DUSP2-ERK1/2 axis in gastric cancer. A Co-transfected with shSKA3 and shDUSP2 rescue EMT and MAPK/ERK related proteins compared with shSKA3 group in MGC-803 and

HGC-27. B Model of SKA3-DUSP2-ERK1/2 axis in gastric cancer

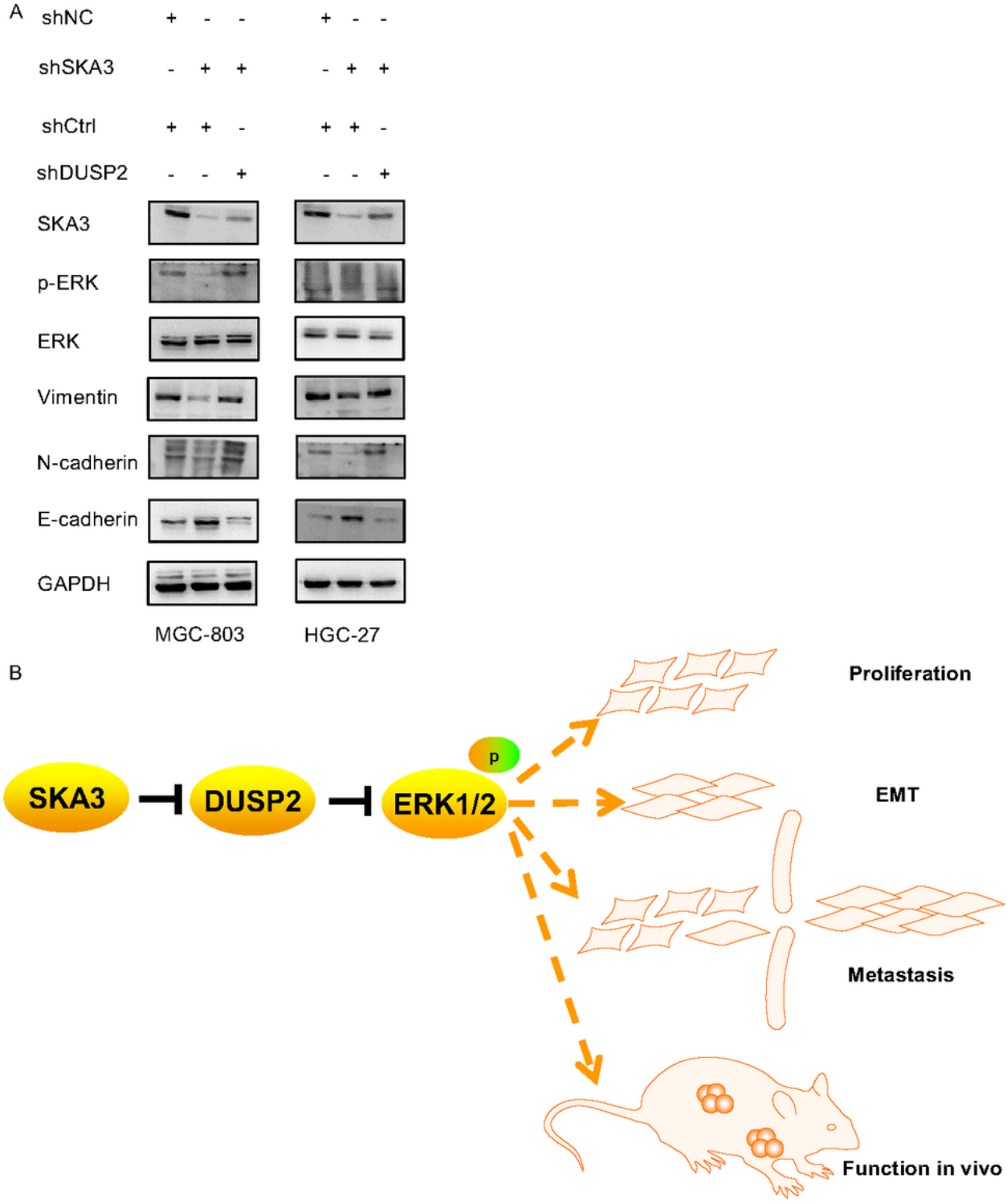

Figure 8

model illustrating SKA3-DUSP2-ERK1/2 axis in gastric cancer. A Co-transfected with shSKA3 and shDUSP2 rescue EMT and MAPK/ERK related proteins compared with shSKA3 group in MGC-803 and HGC-27. B Model of SKA3-DUSP2-ERK1/2 axis in gastric cancer

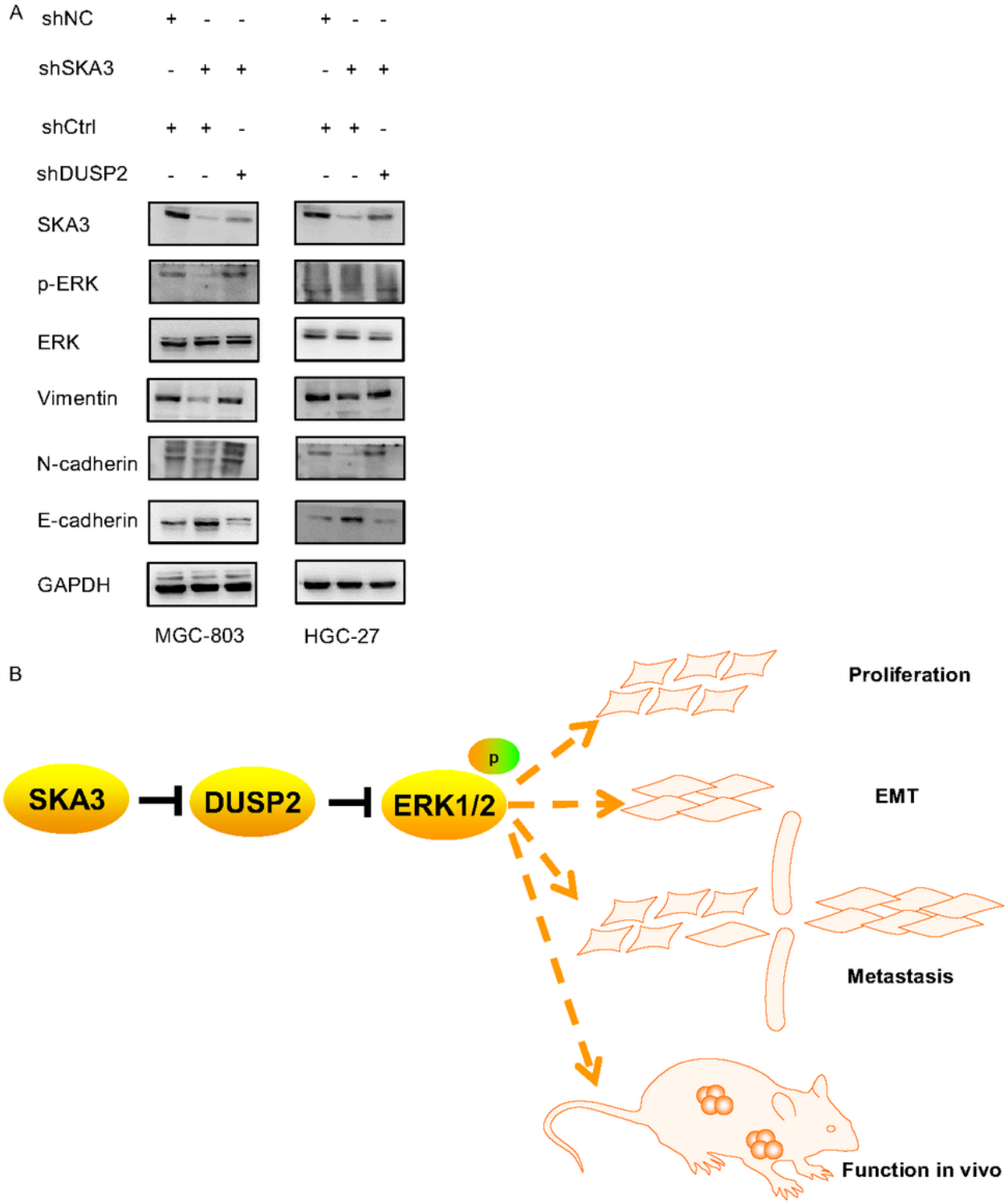

Figure 8

model illustrating SKA3-DUSP2-ERK1/2 axis in gastric cancer. A Co-transfected with shSKA3 and shDUSP2 rescue EMT and MAPK/ERK related proteins compared with shSKA3 group in MGC-803 and HGC-27. B Model of SKA3-DUSP2-ERK1/2 axis in gastric cancer